Exact Form-Factor Results for the Longitudinal Structure Factor of the Massless XXZ Model in Zero Field

Jean-Sébastien Caux[1], Hitoshi Konno[2], Mark Sorrell[3], and Robert Weston[4]

[1] *Institute for Theoretical Physics, Universiteit van Amsterdam, Science Park 904, Postbus 94485, 1090 GL Amsterdam, The Netherlands*

[2] *Department of Mathematics, Hiroshima University, Higashi-Hiroshima 739-8521, Japan*

[3] *Department of Mathematics & Statistics, The University of Melbourne, Parkville, VIC, 3010, Australia*

[4] *Department of Mathematics, Heriot-Watt University, Edinburgh EH14 4AS, UK*

October 31, 2018

Abstract

We consider the XXZ quantum spin chain in its massless, disordered regime at zero field. We derive an exact expression for the two-spinon form-factor of $S^z = \frac{1}{2}\sigma^z$ by taking a limit of the massive XYZ form-factors found by Lashkevich and by Lukyanov and Terras. This result is used to find the two-spinon contribution to the spectral decomposition of the longitudinal structure factor $S^{zz}(k,w)$. We find that this contribution provides an accurate approximation to the full structure factor over a wide range of the anisotropy parameter. The asymptotic behaviour of $S^{zz}(k,w)$ is computed as the upper and lower w thresholds of the two-spinon (w,k) band are approached, and an analysis of the region of validity of this threshold behaviour is performed. Our results reproduce and refine existing threshold behaviour predictions and extend these results to an accurate description throughout the two-spinon continuum.

Dedicated to Professor Michio Jimbo on his sixtieth birthday

1 Introduction

Interacting quantum systems have unique properties when space is one-dimensional [1]. On the one hand, the simple fact that particles cannot avoid each other means that the nature of quantum dynamics is complicated in one dimension. The inevitability of particle interactions means that all excitations are collective ones. In particular, the quasi-free excitations of Fermi liquids in higher dimensions are replaced by the non-perturbative excitations described at low energies by the theory of Tomonaga-Luttinger liquids in one dimension. On the other hand, the tools for dealing with non-perturbative systems are far more sophisticated for one dimension than for higher dimensions. For the class of systems that are quantum integrable, the mathematical toolbox is particularly full.

The most studied interacting, one-dimensional quantum integrable system is the Heisenberg, or XXZ, quantum spin chain [2, 3]

$$H_{XXZ} = -\frac{J}{4}\sum_{i=1}^{N}(\sigma_i^x\sigma_{i+1}^x + \sigma_i^y\sigma_{i+1}^y - \Delta\sigma_i^z\sigma_{i+1}^z) \tag{1.1}$$

with $\Delta = \cos(\pi/(\xi+1))$. This model has two nice properties: many exact non-perturbative results exist for both finite and infinite N (see for example [4, 5] and the many references they contain); and it is experimentally realised. When $J > 0$, the XXZ chain has a massive antiferromagnetic phase for $\Delta > 1$ and is realised for example by $CsCoCl_3$ [6]. When $|\Delta| \leq 1$ the model has a massless disordered phase and has been realised experimentally by frustrated spin ladder systems [7, 8, 9] and, very recently, has become in principle accessible using optical lattices [10]-[14].

In paper [15], we have considered the $N \to \infty$ limit of the Hamiltonian (1.1) in the massless phase with $0 \leq \Delta \leq 1$ (the change in gauge from H_{XXZ} to the Hamiltonian H considered in [15] is given in Section 4 of the current paper). In this phase, the system is a Tomonaga-Luttinger liquid [16, 17] whose fundamental particles are 'spinons': spin-1/2 excitations that can be viewed as domain walls dressed with quantum fluctuations [18]. When $\Delta = 0$ these excitations are non-interacting and are described by free fermions. Away from $\Delta = 0$ the spinons are shaped by the interactions in the bulk, and these interactions can be probed by determining how spinons contribute to correlation functions. The correlation function we have considered in detail in [15] is the longitudinal structure factor (LSF)

$$S^{zz}(k,\omega) = \sum_{j\in\mathbb{Z}} e^{-ikj} \int_{-\infty}^{\infty} dt e^{i\omega t} \langle \mathrm{vac}|S_j^z(t) S_0^z(0)|\mathrm{vac}\rangle \tag{1.2}$$

where $S^z = \frac{1}{2}\sigma^z$. The LSF can be measured directly in neutron scattering experiments (see [19] and references therein). $S^{zz}(k,\omega)$ can be computed by resolving the identity in terms of a complete set of spinon states $\mathbb{I} = \sum_\alpha |\alpha\rangle\langle\alpha|$ and inserting into (1.2) to give the spectral decomposition

$$S^{zz}(k,w) = \sum_\alpha (2\pi)^2 \delta(k - K(\alpha)) \delta(w - W(\alpha)\, |\langle \mathrm{vac}|S_0^z|\alpha\rangle|^2,$$

where $K(\alpha)$ and $W(\alpha)$ are the momentum and energy of the state $|\alpha\rangle$. In our paper [15], we have presented the result for the exact two-spinon contribution to this sum and shown that this contribution is a highly accurate truncation, saturating two independent sum rules to around 99% at $\Delta = 0.5$.

The main purpose of the current paper is to explain the derivation of the results presented in brief in [15]. In particular, we show how the relevant two-spinon form factors $\langle \mathrm{vac}|S_0^z|\alpha\rangle$ are obtained for the massless phase of the XXZ model. The general method that we follow to obtain massless XXZ form-factors is usually called the vertex operator approach (VOA). The VOA for the antiferromagnetic XXZ model is described in detail in [20], where the representation theory of the quantum affine algebra $U_q(\widehat{\mathfrak{sl}}_2)$ plays an essential role. This theoretical framework has been exploited to offer results on dynamical correlation functions of the Heisenberg chain both at the isotropic antiferromagnetic point, where two [21, 22] and four-spinon [23, 24] contributions have been obtained, and for the gapped antiferromagnet, where two-spinon contributions to the transverse correlator were given [25, 26]. In order to extend this approach to deal with the massless regime we follow the strategy proposed in [27]: we use the VOA for the XYZ spin chain in the principal regime, map it to the XYZ disordered regime, and then take a massless limit to the XXZ model.

The XYZ model Hamiltonian is given by

$$H_{XYZ} = -\frac{1}{4} \sum_{i\in\mathbb{Z}} (J_x \sigma_i^x \sigma_{i+1}^x + J_y \sigma_i^y \sigma_{i+1}^y + J_z \sigma_i^z \sigma_{i+1}^z). \tag{1.3}$$

The VOA for the XYZ model was developed in [28, 29]. The role of $U_q(\widehat{\mathfrak{sl}}_2)$ in the XXZ model is taken in the more general XYZ case by the elliptic quantum group of vertex type $\mathcal{A}_{q,p}(\widehat{\mathfrak{sl}}_2)$ [30, 31, 32].

The VOA is directly valid in the principal regime of the XYZ model for which $|J_y| \leq J_x \leq -J_z$. However, as demonstrated in [33], is is possible to map the principal regime to any other region in the phase diagram of the XYZ model. In particular, we can map to the disordered region for which $|J_z| \leq J_y \leq J_x$. A transformation which achieves this is $H^{disord}_{XYZ} = G\, H^{princ}_{XYZ}\, G^\dagger$, where

$$G = \cdots \otimes U_1 \otimes U_0 \otimes U_1 \otimes U_0 \otimes \cdots, \quad U_0 = \frac{-1}{\sqrt{2}} \begin{pmatrix} i & 1 \\ i & -1 \end{pmatrix}, \; U_1 = \frac{1}{\sqrt{2}} \begin{pmatrix} 1 & i \\ -1 & i \end{pmatrix}. \tag{1.4}$$

In this way, it is possible to use the VOA results in the principal regime in order to find form-factors in the disordered region. It remains only to take the limit $J_x \to J_y$ limit, in order to obtain form-factors for the massless XXZ model.

However, things are not quite so simple: while it is true that the VOA to the XYZ model parallels that of the XXZ model, it does differ in one important respect. The explicit multiple-integral expressions for form-factors in the XXZ case are obtained by using a Bosonization technique - more precisely a free-field-representation of the quantum affine algebra $U_q(\widehat{\mathfrak{sl}}_2)$. The problem is that such a free-field representation has not yet been found for the quantum elliptic algebra $\mathcal{A}_{q,p}(\widehat{\mathfrak{sl}}_2)$ relevant to the XYZ model. The reason for this technical problem is ultimately linked to the absence of charge conservation around a vertex in the 8-vertex model associated with the XYZ chain.

This problem has been considered before in the literature, and there are two ways to get around it. The first approach involves mapping the XYZ model to a solid-on-solid (SOS) model, for which a free-field realisation *does* exist (and for which the relevant algebraic structure is the elliptic quantum group of face type $U_{q,p}(\widehat{\mathfrak{sl}}_2)$[34, 35, 36]). This was the method developed and used by Lashkevich and Pugai to obtain expressions for both form-factors and correlation functions in the principal regime XYZ model [37, 38]. The method was extended to higher spin analogues of the XYZ model in [39]. The second approach is applicable specifically to the massless XXZ model; the idea here is to derive and solve a difference equation (a deformed KZ-equation) for correlation functions from the analogous equation for the XYZ model [40], or to construct a field realisation only after having already mapped to the disordered regime and taken the massless limit [27].

In this paper, we take the first approach, the main reason being that simplified expressions for the resulting XYZ two-particle form-factors mapped to the disordered regime are already present in the literature [41]. Our contribution is to take the appropriate massless XXZ scaling limit of these existing results, and to use them to compute the exact two-particle contribution to the longitudinal structure factor.

In Section 2 of this paper, we describe the key components of the VOA to the XYZ model in the principal regime, the map to the disordered regime, and the limit from the existing disordered-regime XYZ form-factor results to our new massless XXZ form-factor expressions. In Section 3, we give the derivation of expression (3.4) for the two-spinon contribution to the longitudinal structure factor $S^{zz}(k, w)$. This was the key result quoted in the earlier paper [15]. In Section 4, we present a detailed quantitative analysis of the structure factor, an analytic derivation of the asymptotic threshold behaviour close to the upper and lower w limits of the two-particle (w, k) continuum, and an analysis of the region of the (w, k) band over which this threshold behaviour is a good practical approximation for different Δ values. We present some concluding remarks in Section 5. Finally, in Appendices A and B, we give the definitions and required properties of elliptic functions, and present an alternative derivation of the mapping of principal form factors to disordered ones.

2 From XYZ to Massless XXZ

A general multiple-integral expression for principal regime XYZ form-factors can be constructed by following the approach of [37, 38]. The case of the form-factor of the operator σ^z is considered in detail in the paper [38], and the author demonstrates a technique that enables him to obtain an expression for this form-factor which involves no integrals. This approach is extended to σ^x and σ^y form-factors by Lukyanov and Terras in [41]. Using the mapping mentioned in the previous section these authors present results directly in the disordered region of the XYZ model. In this section, we review these results and take the appropriate scaling limit to the massless XXZ model. This limit is different to the sine-Gordon limit considered in [41].

2.1 The XYZ model in the principal regime

The XYZ Hamiltonian is derived from the 8-vertex model elliptic R matrix [33] given by

$$R(u) = \rho(u) \begin{pmatrix} a(u) & & & d(u) \\ & b(u) & c(u) & \\ & c(u) & b(u) & \\ d(u) & & & a(u) \end{pmatrix} \tag{2.1}$$

with

$$a(u) = \mathrm{snh}(\lambda(1-u)),\ b(u) = \mathrm{snh}(\lambda u),\ c(u) = \mathrm{snh}(\lambda),\ d(u) = k\mathrm{snh}(\lambda(1-u))\mathrm{snh}(\lambda u)\mathrm{snh}(\lambda).$$

Here $\mathrm{snh}(u) = -i\mathrm{sn}(iu)$ is the Jacobi elliptic function with modulus k. The definitions, relations between and required properties of all elliptic functions used in this paper can be found in Appendix A. Let K, K' be the corresponding complete elliptic integrals given in Appendix A. We use the variables

$$x^{2r} = e^{-\frac{\pi K'}{K}}, \quad x = e^{-\frac{\pi\lambda}{2K}}, \quad \zeta = x^u,$$

from which definition it follows that $\lambda = K'/r$. We also define $p = e^{-\frac{4\pi K}{K'}}$ and $\delta = \frac{\lambda}{K}$, and sometimes use $\xi = r - 1$ when connecting to the results of [41]. The principal regime is given by $0 < x^r < x < \zeta < 1$. We choose the scalar function $\rho(u)$ as follows.

$$\begin{aligned}
\rho(u) &= x^{1-r/2}\frac{(x^{4r};x^{4r})_\infty}{(x^{2r};x^{2r})_\infty^2}\frac{\Theta_{x^{4r}}(x^{2r}x^2)\Theta_{x^{4r}}(x^{2r}\zeta^{-2})}{\Theta_{x^{4r}}(x^2\zeta^{-2})}\frac{g(\zeta^{-2})}{g(\zeta^2)}, \\
g(z) &= \frac{(x^2z;x^4,x^{2r})_\infty(x^{2r}x^2z;x^4,x^{2r})_\infty}{(x^4z;x^4,x^{2r})_\infty(x^{2r}z;x^4,x^{2r})_\infty}, \\
(z;q_1,\cdots,q_m)_\infty &= \prod_{n_1,\cdots,n_m=0}^{\infty}(1-zq_1^{n_1}\cdots q_m^{n_m}), \\
\Theta_q(z) &= (q;q)_\infty(z;q)_\infty(q/z;q)_\infty.
\end{aligned}$$

This form of the R-matrix coincides with that used in [38] except for a minus sign in $d(u)$. However, our notation differs slightly: most importantly, our p is not equal to the p of [38]. A full dictionary between our notation and that of both [38] and [41] is given in Table 1.

For $V = \mathbb{C}v_+ \oplus \mathbb{C}v_-$, we regard $R(u)$ as a linear map on $V \otimes V$ by

$$R(u)v_{\varepsilon_1} \otimes v_{\varepsilon_2} = \sum_{\varepsilon_1',\varepsilon_2=\pm} R^{\varepsilon_1\varepsilon_2}_{\varepsilon_1'\varepsilon_2'}(u)v_{\varepsilon_1'} \otimes v_{\varepsilon_2'}.$$

Table 1: A Dictionary of Notation

This paper	Reference [38]	Reference [41]
u	u	-
λ	-	-
r	r	$\frac{1}{1-\eta}$
$\delta = \frac{\lambda}{K}$	$\frac{2\epsilon}{\pi}$	δ
$\xi = r - 1$	$r - 1$	$\xi = \frac{\eta}{1-\eta}$
$x = e^{-\frac{\pi\lambda}{2K}}$	$x = e^{-\epsilon}$	$e^{-\pi\delta/2}$
$x^{2r} = e^{-\frac{\pi K'}{K}}$	$p = x^{2r}$	$e^{-\pi\delta(\xi+1)}$
$p = e^{-\frac{4\pi K}{K'}}$	$e^{\frac{-2\pi^2}{\epsilon r}}$	$p = e^{-\frac{4\pi}{\delta(\xi+1)}}$

Let V_i $(i = 0, 1, .., N)$ denote $N+1$ copies of V and regard $R_{ij}(u)$ as a linear map on $V_N \otimes \cdots \otimes V_1 \otimes V_0$ acting on the i-th and j-th tensor components as $R(u)$ and on the other components trivially. We define the finite transfer matrix $T(u)$ by

$$T(u) \quad = \quad \mathrm{tr}_V R_{N0}(u) R_{N-10}(u) \cdots R_{10}(u).$$

Then one can verify that in the infinite N limit the XYZ Hamiltonian (1.3) is obtained as

$$H_{XYZ} = -\frac{J\mathrm{sn}(\lambda, k')\mathrm{cn}(\lambda, k')}{2\lambda} \frac{d}{du} \ln T(u)\Big|_{u=0} + \text{constant}, \tag{2.2}$$

with $k' = \sqrt{1-k^2}$ and

$$\begin{aligned} J_x &= J\left(\mathrm{cn}^2(\lambda, k') + k\mathrm{sn}^2(\lambda, k')\right), \\ J_y &= J\left(\mathrm{cn}^2(\lambda, k') - k\mathrm{sn}^2(\lambda, k')\right), \\ J_z &= -J\mathrm{dn}(\lambda, k'). \end{aligned} \tag{2.3}$$

2.2 The vertex operator approach to the XYZ model in the principal regime

The vertex operator approach to the infinite-lattice massive antiferromagnetic XXZ model was developed in [42] and is described in detail in the book [20]. This approach was then extended to the principal regime XYZ model in [28]-[32]. The essence of the approach is to identify the transfer matrix, the space on which it acts, and local operators in terms of the representation theory of the underlying symmetry algebra. In the XXZ case, this algebra is the quantum affine algebra $U_q\big(\widehat{\mathfrak{sl}}_2\big)$; in the XYZ case it is the elliptic algebra $\mathcal{A}_{q,p}(\widehat{\mathfrak{sl}}_2)$ (beware that the (q,p) indicated in the name $\mathcal{A}_{q,p}(\widehat{\mathfrak{sl}}_2)$ do not correspond directly to the notation of the current paper - in fact we have $(q,p) = (-x, x^{2r})$). In this section and Appendix B, we give a brief outline of the key features of the approach relevant to the present work. We refer the interested reader to the original articles cited above and [39] for further details.

The lattice transfer matrix of the infinite-size principal-regime XYZ model acts on the infinite tensor product space $\cdots \otimes V \otimes V \otimes V \otimes V \otimes \cdots$ with antiferromagnetic boundary conditions at plus and minus infinity. Let us choose to label the position of our spin-chain sites as $\cdots, 2, 1, 0, -1, -2, \cdots$.

Then the two antiferromagnetic boundary conditions we consider are labelled by $j = 0$ or $j = 1$ and correspond to considering only those states which have the spin at site i, denote $\varepsilon(i)$, restricted to $\bar{\varepsilon}^{(j)}(i) = (-1)^{i+j+1}$ for $|i| >> 0$. More precisely, we introduce the space of states $\mathcal{H}^{(j)}$ $(j = 0, 1)$ as a half of the infinite tensor space with the antiferromagnetic boundary condition j. Namely

$$\mathcal{H}^{(j)} \;:=\; \mathrm{Span}_{\mathbb{C}} \left\{ \cdots \otimes v_{\varepsilon(1)} \otimes v_{\varepsilon(0)} \mid \varepsilon(i) = \pm,\ \varepsilon(i) = \bar{\varepsilon}^{(j)}(i) \text{ for } i \gg 0 \right\}, \tag{2.4}$$

where $v_+ = \begin{pmatrix} 1 \\ 0 \end{pmatrix}, v_- = \begin{pmatrix} 0 \\ 1 \end{pmatrix}$. The starting point of the vertex operator approach is to identify the space of states $\mathcal{H}^{(j)}$ with the level-1 highest weight modules $V(\Lambda_j)$ $(j = 0, 1)$ of the algebra $\mathcal{A}_{q,p}(\widehat{\mathfrak{sl}}_2)$, where Λ_j denotes the fundamental weight of $\widehat{\mathfrak{sl}}_2$. Then, the total infinite tensor product space is identified with the tensor product

$$\mathcal{F}^{(j)} := \mathcal{H}^{(j)} \otimes \mathcal{H}^{*(j)} \simeq \mathrm{End}(\mathcal{H}^{(j)}). \tag{2.5}$$

The transfer matrix of the XYZ model and local operators are then identified in terms of certain vertex operators that act on the space (2.4). The relevant 'type I' vertex operators are maps involving both $\mathcal{H}^{(j)}$ and a finite-dimensional $\mathcal{A}_{q,p}(\widehat{\mathfrak{sl}}_2)$ evaluation module $V_u = V \otimes \mathbb{C}[\zeta, \zeta^{-1}]$. They are $\mathcal{A}_{q,p}(\widehat{\mathfrak{sl}}_2)$ homomorphisms of the form

$$\Phi^{(1-j,j)}(u) : \mathcal{H}^{(j)} \longrightarrow \mathcal{H}^{(1-j)} \otimes V_u, \tag{2.6}$$

whose components $\Phi^{(1-j,j)}_{\pm}(u)$ are defined by

$$\Phi^{(1-j,j)}(u) = \sum_{\varepsilon=\pm} \Phi^{(1-j,j)}_{\varepsilon}(u) \otimes v_{\varepsilon}.$$

The transfer matrix of the XYZ model is identified with the map $T(u) : \mathcal{F}^{(j)} \to \mathcal{F}^{(1-j)}$ defined by

$$T(u) = \sum_{\varepsilon=\pm} \Phi^{(1-j,j)}_{\varepsilon}(u) \otimes \Phi^{(j,1-j)}_{-\varepsilon}(u)^t, \tag{2.7}$$

where t denotes transpose. The XYZ Hamiltonian is then identified as

$$-\frac{J\mathrm{sn}(\lambda, k')\mathrm{cn}(\lambda, k')}{2\lambda} \frac{d}{du} \ln T(u)\Big|_{u=0}. \tag{2.8}$$

Now we consider the 2×2 matrix $E_{\varepsilon,\varepsilon'}$ that acts as $E_{\varepsilon,\varepsilon'} v_\alpha = \delta_{\alpha,\varepsilon'} v_\varepsilon$ at site 0 of the lattice. This local operator is realised as an operator on $\mathcal{H}^{(j)}$ in the vertex operator approach as

$$\mathcal{O}(E_{\varepsilon\varepsilon'})^{(j)} = \Phi^{(j,1-j)}_{-\varepsilon}(u-1)\Phi^{(1-j,j)}_{\varepsilon'}(u)\Big|_{u=0}. \tag{2.9}$$

Then the spin operator σ^x for example is realised as $\mathcal{O}(\sigma^x)^{(j)} = \mathcal{O}(E_{+-})^{(j)} + \mathcal{O}(E_{-+})^{(j)}$.

The vacuum eigenvector of the transfer matrix $T(u)$ is denoted by $|\mathrm{vac}; pr\rangle^{(j)} \in \mathcal{F}^{(j)}$ and defined by

$$T(u)|\mathrm{vac}; pr\rangle^{(j)} = |\mathrm{vac}; pr\rangle^{(1-j)}. \tag{2.10}$$

This eigenvector[1] has a very simple form in the vertex operator picture, and is constructed in terms of a certain grading operator $H^{(j)}$ that acts on $\mathcal{H}^{(j)}$. More precisely, we define $H^{(j)} = -\frac{1}{2}\rho + \frac{j}{4}$, where $\rho = \Lambda_0 + \Lambda_1$, and identify

$$|\mathrm{vac}; pr\rangle^{(j)} = \frac{1}{(Z^{(j)})^{\frac{1}{2}}} x^{2H^{(j)}},$$

where we are regarding $\mathcal{F}^{(j)} \simeq \mathrm{End}(\mathcal{H}^{(j)})$. Namely, $T(u)$ acts on $f \in \mathrm{End}(\mathcal{H}^{(j)})$ as

$$T(u)f = \sum_{\varepsilon=\pm} \Phi_{\varepsilon}^{(1-j,j)}(u) \circ f \circ \Phi_{-\varepsilon}^{(j,1-j)}(u), \tag{2.11}$$

see [20]. The normalisation is defined by the $\widehat{\mathfrak{sl}}_2$ principal character

$$Z^{(j)} = \mathrm{Tr}_{\mathcal{H}^{(j)}}(x^{4H^{(j)}}) = \frac{1}{(x^2; x^4)_\infty}, \tag{2.12}$$

and is chosen such that ${}^{(j)}\langle \mathrm{vac}; pr|\mathrm{vac}; pr\rangle^{(j)} = 1$. Here the inner product of two elements $f, g \in \mathrm{End}(\mathcal{H}^{(j)})$ is defined by $(f, g) = \mathrm{Tr}_{\mathcal{H}^{(j)}}(f \circ g)$. We denote a vector in $\mathcal{F}^{(j)} = \mathcal{H}^{(j)} \otimes \mathcal{H}^{*(j)}$ by a ket vector in this section, but it should be understood that it is identified with an operator in $\mathrm{End}(\mathcal{H}^{(j)})$ whenever one considers an action of the vertex operators on it. In what follows, we refer to arguments based on the identification $\mathcal{F}^{(j)} \cong \mathrm{End}(\mathcal{H}^{(j)})$ as the 'vertex operator picture'.

The reader may at this point be thinking that the vertex operator approach is wholly algebraic and formal, but in fact $H^{(j)}$, $\Phi_\varepsilon(u)$ and $Z^{(j)}$ have a direct lattice interpretation in terms of the 8-vertex model: the operator $H^{(j)}$ is identified with Baxter's corner-transfer-matrix Hamiltonian, $\Phi_\varepsilon(u)$ with the half-transfer matrix, and $Z^{(j)}$ with the partition function. In fact, it was Baxter's observation [33] that it it possible to express the partition function in terms of the corner-transfer-matrix Hamiltonian as in Equation (2.12), and the subsequent observation that this partition function was related to the $\widehat{\mathfrak{sl}}_2$ principal character, that were the starting points for the development of the vertex operator approach.

In order to construct other eigenstates of the operator (2.7) it is necessary to introduce a new 'type II' vertex operator $\Psi^{*(1-j,j)}(u)$, defined as the map

$$\Psi^{*(1-j,j)}(u) : V_u \otimes \mathcal{H}^{(j)} \longrightarrow \mathcal{H}^{(1-j)},$$

with components $\Psi_{\pm}^{*(1-j,j)}(u)$ specified by

$$\Psi_{\varepsilon}^{*(1-j,j)}(u) = \Psi^{*(1-j,j)}(u)\,(v_\varepsilon \otimes \cdot)\,.$$

The full list of properties of both type I and type II vertex operators can be found in [38]. One property that we require in the current paper is the commutation relation of type I and type II vertex operators:

$$\Phi_{\varepsilon_1}^{(j,1-j)}(u_1)\Psi_{\varepsilon_2}^{*(1-j,j)}(u_2) = \tau(u_1 - u_2)\Psi_{\varepsilon_2}^{*(j,1-j)}(u_2)\Phi_{\varepsilon_1}^{(1-j,j)}(u_1), \tag{2.13}$$

where the function $\tau(u)$ is given by [38]

$$\tau(u) = i\frac{\vartheta_1\left(\frac{1}{4} - \frac{u}{2}, p^{\frac{r}{4}}\right)}{\vartheta_1\left(\frac{1}{4} + \frac{u}{2}, p^{\frac{r}{4}}\right)}. \tag{2.14}$$

[1] We are using the term eigenvector loosely: $|\mathrm{vac}; pr\rangle^{(j)}$ is a true eigenvector only of $T^2(u)$.

Our convention for theta functions is given in Appendix A.

Let us consider a state defined by

$$|\theta_1,\theta_2;pr\rangle^{(j)}_{\varepsilon_1,\varepsilon_2}=\Psi^{*(j,1-j)}_{\varepsilon_2}(i\theta_2/\pi)\Psi^{*(1-j,j)}_{\varepsilon_1}(i\theta_1/\pi)|\mathrm{vac};pr\rangle^{(j)}.$$

It then follows immediately from (2.13), (2.7) and (2.11) that we have

$$T(u)|\theta_1,\theta_2;pr\rangle^{(j)}_{\varepsilon_1,\varepsilon_2}=\tau(u-i\theta_1/\pi)\tau(u-i\theta_2/\pi)|\theta_1,\theta_2;pr\rangle^{(1-j)}_{\varepsilon_1,\varepsilon_2}. \tag{2.15}$$

Hence, we may create a new eigenstate of $T(u)$, i.e., an excited state with an eigenvalue $\tau(u-i\theta_1/\pi)\tau(u-i\theta_2/\pi)$, by acting on the vacuum with the type II vertex operators. More precisely, the type II vertex operators $\Psi^{*(1-j,j)}_{\varepsilon}(u)$ are identified with the creation operators of quasi-particle (spinon) excitations with rapidity $\theta=-i\pi u$ and spin ε. The $2n$-spinon state (spinons are always excited in pairs) is given by

$$|\theta_1,\cdots,\theta_{2n};pr\rangle^{(j)}_{\varepsilon_1,\cdots,\varepsilon_{2n}}=\Psi^{*(j,1-j)}_{\varepsilon_{2n}}\left(i\theta_{2n}/\pi\right)\cdots\Psi^{*(1-j,j)}_{\varepsilon_1}\left(i\theta_1/\pi\right)|\mathrm{vac};pr\rangle^{(j)}. \tag{2.16}$$

From (2.15), one finds that the eigenvalue of $T(u)$ per spinon is $\tau(u-i\theta/\pi)$. Then from (2.8), one can deduce that the pseudomomentum $k(\theta)$ and energy $\omega(\theta)$ of a spinon state in the principal XYZ model are

$$\begin{aligned}e^{ik(\theta)}&=\tau(-i\theta/\pi),\\ \omega(\theta)&=\frac{J\mathrm{sn}(\lambda,k')\mathrm{cn}(\lambda,k')}{2\lambda}\frac{\partial}{\partial u}\ln\tau(u-i\theta/\pi)\Big|_{u=0}.\end{aligned}$$

Hence we obtain

$$k(\theta)=\mathrm{am}\left(\frac{2I'\theta}{\pi},k_I\right)+\frac{\pi}{2}, \tag{2.17}$$

$$\begin{aligned}\omega(\theta)&=\frac{JI'\mathrm{sn}(\lambda,k')\mathrm{cn}(\lambda,k')}{\lambda}\mathrm{dn}\left(\frac{2I'\theta}{\pi},k_I\right)\\ &=\frac{JI'\mathrm{sn}(\lambda,k')\mathrm{cn}(\lambda,k')}{\lambda}\sqrt{1-k_I^2\cos^2(k(\theta))}.\end{aligned} \tag{2.18}$$

Here we have introduced new complete elliptic integrals I,I' by

$$x=e^{-\frac{\pi I'}{I}}$$

and denote by k_I, k_I' the corresponding moduli (that is, we now consider elliptic function with nome x as opposed to the original functions involved in the R-matrix which had nome x^{2r}). The symbols $\mathrm{sn}(u,k_I),\mathrm{dn}(u,k_I),\mathrm{am}(u,k_I)$ denote Jacobi's elliptic function with modulus k_I. In deriving (2.17) and (2.18), we have used the identity between elliptic functions of different nomes given in Equation (A.7). Expressions (2.17) and (2.18) for spinon pseudomomentum and energy are consistent with the results of [43].

The 2n-spinon form factor of the local operator $E_{\varepsilon,\varepsilon'}$ can now be expressed in the vertex operator picture as the following trace:

$$\begin{aligned}&{}^{(j)}\langle\mathrm{vac};pr|E_{\varepsilon,\varepsilon'}|\theta_1,\cdots,\theta_{2n};pr\rangle^{(j)}_{\varepsilon_1,\cdots,\varepsilon_{2n}}\\ &=\frac{1}{Z}\mathrm{tr}_{\mathcal{H}^{(j)}}\Big(x^{4H^{(j)}}\mathcal{O}(E_{\varepsilon,\varepsilon'})^{(j)}\Psi^{*(j,1-j)}_{\varepsilon_{2n}}(i\theta_{2n}/\pi)\Psi^{*(1-j,j)}_{\varepsilon_{2n-1}}(i\theta_{2n-1}/\pi)\cdots\Psi^{*(1-j,j)}_{\varepsilon_1}(i\theta_1/\pi)\Big).\end{aligned} \tag{2.19}$$

The massive, antiferromagnetic XXZ model corresponds to the $r \to \infty$ ($k \to 0$) limit of the above picture. In this limit the above trace can be computed directly in terms of the free-field realisation of $U_q\big(\widehat{\mathfrak{sl}}_2\big)$ [20]. However, there is no known free-field realisation for the general elliptic case. This problem was overcome in [37, 38] by mapping the 8-vertex model to the SOS model using Baxter's intertwiners. A free field realisation *does* exist for the SOS model [44, 45, 34, 35] and this was used to produced an integral expression for (2.19) which may be found in [38].

2.3 The map to the disordered regime

Any regime of the XYZ model can be obtained from the principal regime by a suitable gauge transformation [33]. In this section, we construct such a transformation in terms of the following matrices

$$U_0 = \frac{-1}{\sqrt{2}}\begin{pmatrix} i & 1 \\ i & -1 \end{pmatrix}, \quad U_1 = \frac{1}{\sqrt{2}}\begin{pmatrix} 1 & i \\ -1 & i \end{pmatrix}.$$

The adjoint action of these matrices on Pauli matrices is given by

$$U_0(\sigma^x, \sigma^y, \sigma^z)U_0^{-1} = (\sigma^y, \sigma^z, \sigma^x), \quad U_1(\sigma^x, \sigma^y, \sigma^z)U_1^{-1} = (\sigma^y, -\sigma^z, -\sigma^x). \tag{2.20}$$

We consider the following gauge transformations.

$$\widetilde{R}(u) = (U_1 \otimes U_0)R(u)(U_0^{-1} \otimes U_1^{-1}) = (U_0 \otimes U_1)R(u)(U_1^{-1} \otimes U_0^{-1}). \tag{2.21}$$

Note that a similar gauge transformation has been discussed in [27]. The difference is due to the shift $\lambda \to \lambda - 2iK$ made in sec.2.4 of [27].

Now define the infinite tensor product G_j ($j = 0, 1$) by

$$G_j = \cdots \otimes U_{1-j} \otimes U_j \otimes U_{1-j} \otimes U_j \otimes \cdots . \tag{2.22}$$

where U_j acts at even sites of our infinite product space. Then it follows that with H_{XYZ} given by (1.3), we have

$$H_{XYZ}^{dis} = G_j H_{XYZ} G_j^{-1} = -\frac{1}{4}\sum_{i\in\mathbb{Z}}(J_x^{dis}\sigma_i^x\sigma_{i+1}^x + J_y^{dis}\sigma_i^y\sigma_{i+1}^y + J_z^{dis}\sigma_i^z\sigma_{i+1}^z),$$
$$\text{where } \ J_x^{dis} = -J_z, \ \ J_y^{dis} = J_x, \ \ J_z^{dis} = -J_y.$$

With the parametrisation (2.3), we have $|J_y| \le J_x \le -J_z$ which corresponds to the principle regime. Hence, we have $|J_z^{dis}| \le J_y^{dis} \le J_x^{dis}$ which corresponds to the disordered regime [33].

In order to apply the gauge transformation to the space of states $\mathcal{H}^{(\ell)}$ ($\ell = 0, 1$), let us devide G_j into two parts in the following way.

$$G_j = \mathcal{G}_j \otimes \widetilde{\mathcal{G}}_{1-j}$$

with

$$\mathcal{G}_j = \cdots \otimes U_j \otimes U_{1-j} \otimes U_j, \quad \widetilde{\mathcal{G}}_j = U_j \otimes U_{1-j} \otimes U_j \otimes \cdots$$

Here we assume the rightmost U_j of $\mathcal{G}_j$ acts on the 0-th site of our infinite product space.

By transforming $\mathcal{H}^{(\ell)}$ by $\mathcal{G}_j$, one finds the following two spaces.

$$\mathcal{H}^{(0)}_{dis} := \mathrm{Span}_{\mathbb{C}}\{\cdots\otimes w_0\otimes w_0\otimes w_0\otimes\cdots\otimes w_{j_1}\otimes w_{j_0} \mid j_0,j_1,\cdots\in\{0,1\}\ \},$$
$$\mathcal{H}^{(1)}_{dis} := \mathrm{Span}_{\mathbb{C}}\{\cdots\otimes w_1\otimes w_1\otimes w_1\otimes\cdots\otimes w_{j_1}\otimes w_{j_0} \mid j_0,j_1,\cdots\in\{0,1\}\ \},$$

where w_0, w_1 denote the eigenvectors of σ^x given by

$$w_0 = \frac{1}{\sqrt{2}}\begin{pmatrix}1\\1\end{pmatrix}, \quad w_1 = \frac{1}{\sqrt{2}}\begin{pmatrix}1\\-1\end{pmatrix}.$$

Namely we have

$$\mathcal{H}^{(j)}_{dis} = \mathcal{G}_{j+\ell}\mathcal{H}^{(1-\ell)} \quad (\ell = 0,1). \tag{2.23}$$

Here and hereafter index $j+\ell$ should be understood in mod 2. We regard $\mathcal{H}^{(j)}_{dis}$ $(j=0,1)$ as the spaces of states in the disordered regime. We also set $\mathcal{H}^{*(j)}_{dis} = \widetilde{\mathcal{G}}_{1+j+\ell}\mathcal{H}^{*(1-\ell)}$ and define the total space $\mathcal{F}^{(j)}_{dis} = G_{j+\ell}\mathcal{F}^{(1-\ell)} = \mathcal{H}^{(j)}_{dis}\otimes\mathcal{H}^{*(j)}_{dis}$.

Accordingly, eigenstates of H^{dis}_{XYZ} are obtained by acting with G_j on the eigenstates of H_{XYZ} and have the same energy. Noting the duplication (2.23), we have a new vacuum vector $|\mathrm{vac}\rangle^{(j)}$ in $\mathcal{F}^{(j)}_{dis}$ expressed in two ways as

$$|\mathrm{vac}\rangle^{(j)} = G_{j+\ell}|\mathrm{vac};pr\rangle^{(1-\ell)}$$

with $\ell = 0,1$.

2.4 The massless XXZ limit

The massless XXZ Hamiltonian is obtained by taking the limit $x\to 1$ $(K\to+\infty)$ of the disordered Hamiltonian H^{dis}_{XYZ} while keep r fixed. This corresponds to the following limits of the various elliptic parameters:

$$K'\to\frac{\pi}{2},\ \ k\to 1,\ \ k'\to 0,\ \ \delta\to 0_+,\ \ \lambda\to\frac{\pi}{2r}.$$

Corresponding to this limit, we have

$$J_x\to J, \quad J_y\to J\cos\left(\frac{\pi}{r}\right), \quad J_z\to -J.$$

Defining $\Delta = \cos\left(\frac{\pi}{r}\right)$, we then have

$$H^{dis}_{XYZ}\to -\frac{J}{4}\sum_{i\in\mathbb{Z}}(\sigma^x_i\sigma^x_{i+1}+\sigma^y_i\sigma^y_{i+1}-\Delta\sigma^z_i\sigma^z_{i+1}),$$

which is the Hamiltonian of the massless XXZ model.

In order to obtain the dispersion relation for the massless XXZ model, let us set $\theta_+ = \beta$ and $\theta_- = \beta - \frac{2\pi}{\delta}$. One should note $p^{\frac{r}{4}} = e^{-\frac{\pi}{\delta}}$. Then it follows from (2.17) and (2.18) that we have

$$\begin{aligned} k(\theta_\pm) &= \mathrm{am}\left(\frac{2I'\beta}{\pi}, k_I\right)\pm\frac{\pi}{2},\\ \omega(\theta_\pm) &= \frac{JI'\mathrm{sn}(\lambda,k')\mathrm{cn}(\lambda,k')}{\lambda}\mathrm{dn}\left(\frac{2I'\beta}{\pi},k_I\right).\end{aligned}$$

The above massless XXZ limit implies

$$I \to +\infty, \;\; I' \to \frac{\pi}{2}, \;\; k_I \to 1, \;\; k'_I \to 0.$$

Defining $\kappa(\beta)$ by

$$\kappa(\beta) := 2\arctan(e^{\beta}),$$

we find the pseudomomentum $k(\theta_\pm)$ and energy $\omega(\theta_\pm)$ of a spinon of the massless XXZ model are given by

$$\begin{aligned} \lim k(\theta_+) &= \kappa(\beta), \quad \lim k(\theta_-) = \kappa(\beta) - \pi \\ \lim \omega(\theta_\pm) &= \frac{v_F}{\cosh(\beta)} = v_F |\sin \kappa(\beta)|. \end{aligned}$$

Here v_F denotes the Fermi velocity given by

$$v_F = \frac{Jr}{2}\sin\left(\frac{\pi}{r}\right) = \frac{\pi J}{2}\frac{\sqrt{1-\Delta^2}}{\arccos(\Delta)}. \tag{2.24}$$

In deriving these limits we have made use of the conjugate modulus transformation for dn given by Equation (A.5) and of the limits of elliptic functions given by Equations (A.8) and (A.9).

For β real, the range of $2\arctan(e^{\beta})$ is $(0, \pi)$, and so the + parametrisation gives us right-moving spinons occupying half the first Brillouin zone, and the - parametrisation gives us left-moving spinons occupying the other half. However, as we shall discuss in Section 3, spinons come only in pairs, and right-moving spinons are alone sufficient to span the complete Hilbert space of the quantum spin chain.

2.4.1 The sine-Gordon Limit

In [41], the sine-Gordon theory is discussed by taking a similar $x \to 1$ scaling limit of the XYZ model. It is interesting to compare our massless XXZ limit with this relativistic field theory limit. The approach of [41] involves shifting the rapidity in a different way: as $\theta = \vartheta - \frac{\pi}{\delta}$ (we here use ϑ to indicate the parameter denoted by θ in [41]). Then, with a slightly different normalisation of the Hamiltonian, the momentum p and the excitation energy ε of the quantised soliton are given in [41] by

$$\begin{aligned} e^{ip(\vartheta)} &= \tau(-i\vartheta/\pi + i/\delta) = \frac{\vartheta_4\left(\frac{1}{4} + \frac{i\vartheta}{2\pi}, p^{\frac{r}{4}}\right)}{\vartheta_4\left(\frac{1}{4} - \frac{i\vartheta}{2\pi}, p^{\frac{r}{4}}\right)}, \\ \varepsilon(\vartheta) &= \frac{\partial}{\partial\vartheta} p(\theta). \end{aligned}$$

Then in the same scaling limit $x \to 1$ as above together with the limit that the lattice spacing $\epsilon \to 0$, the dispersion relation for massive relativistic particles is given in [41] as

$$\begin{aligned} \lim \frac{p(\vartheta)}{\epsilon} &= M \sinh\vartheta, \\ \lim \frac{\varepsilon(\vartheta)}{\epsilon} &= M \cosh\vartheta, \end{aligned}$$

where the mass M is given by

$$M = \lim \frac{2e^{-\frac{\pi}{\delta}}}{\epsilon}.$$

This sine-Gordon limit is different to our massless XXZ limit and was used in [41] in order to connect lattice and field theory operators.

2.5 Form factors in the disordered regime

In the same way that vacuum vectors in the disordered regime were constructed in Section 1.3, excited states of H^{dis}_{XYZ} are given by

$$|\theta_1, \cdots, \theta_{2n}\rangle^{(j)}_{\varepsilon_1,\cdots,\varepsilon_{2n}} = G_{j+\ell}|\theta_1, \cdots, \theta_{2n}; pr\rangle^{(1-\ell)}_{\varepsilon_1,\cdots,\varepsilon_{2n}}$$

in $\mathcal{F}^{(j)}_{dis}$ with $\ell = 0, 1$. Hence a form factor of a local operator acting on the site 0 for the disordered regime is given by

$${}^{(j)}\langle \mathrm{vac}|E_{\varepsilon,\varepsilon'}|\theta_1, \cdots, \theta_{2n}\rangle^{(j)}_{\varepsilon_1,\cdots,\varepsilon_{2n}} = {}^{(1-\ell)}\langle \mathrm{vac}; pr|U^{-1}_{j+\ell}E_{\varepsilon,\varepsilon'}U_{j+\ell}|\theta_1, \cdots, \theta_{2n}; pr\rangle^{(1-\ell)}_{\varepsilon_1,\cdots,\varepsilon_{2n}}. \tag{2.25}$$

The correspondingly gauge transformed Pauli operators acting at site 0 of the lattice are given by

$$U^{-1}_{j+\ell}(\sigma^x, \sigma^y, \sigma^z)U_{j+\ell} = ((-)^{j+\ell}\sigma^z, \sigma^x, (-)^{j+\ell}\sigma^y).$$

A derivation of the formula (2.25) in the vertex operator picture is given in Appendix B.

As we mentioned above, a general integral formula for the principal form factors appearing on the right-hand-side of Equation (2.25) can be found in [38]. Furthermore, this integral was there performed explicitly in the case when the local operator was σ^z - see (3.14)-(3.16) of [38]. This same method was then used to compute the integrals associated with the other Pauli operators in [41] and a summary of all cases can be found in Appendix A of [41] (where the results are presented directly in the disordered regime). Let us define the function

$$f(z_1, z_2)^{a,b}_{c,d} := \frac{F_0\,\overline{G}(z_1 - z_2, p)\,\vartheta_a(0, p^{\frac{1}{2}})\vartheta_b(\frac{z_1+z_2}{2\pi i}, p^{\frac{\xi+1}{2}})}{\vartheta_c(\frac{z_1}{2\pi i} - \frac{1}{4}, p^{\frac{\xi+1}{4}})\vartheta_c(\frac{z_2}{2\pi i} - \frac{1}{4}, p^{\frac{\xi+1}{4}})\vartheta_d(\frac{z_1-z_2+i\pi}{2\pi i\xi}, p^{\frac{\xi+1}{2\xi}})} \tag{2.26}$$

where F_0 and $\overline{G}(z, p)$ are defined in Appendix A of [41], and we now use the notation $r = \xi + 1$. The results of Appendix A of [41] may be expressed succinctly as

$$\begin{aligned}
{}^{(j)}\langle \mathrm{vac}|\sigma^x|\theta_1, \theta_2\rangle^{(j)}_{\pm,\mp} &= (-1)^j f(\theta_1 + \frac{\pi}{\delta}, \theta_2 + \frac{\pi}{\delta})^{4,4}_{4,1} \pm f(\theta_1 + \frac{\pi}{\delta}, \theta_2 + \frac{\pi}{\delta})^{4,1}_{4,4}, \\
{}^{(j)}\langle \mathrm{vac}|\sigma^y|\theta_1, \theta_2\rangle^{(j)}_{\pm,\pm} &= -f(\theta_1 + \frac{\pi}{\delta}, \theta_2 + \frac{\pi}{\delta})^{3,3}_{4,2} \pm (-1)^{j+1} f(\theta_1 + \frac{\pi}{\delta}, \theta_2 + \frac{\pi}{\delta})^{3,2}_{4,3}, \\
{}^{(j)}\langle \mathrm{vac}|\sigma^z|\theta_1, \theta_2\rangle^{(j)}_{\pm,\pm} &= i(-1)^j f(\theta_1 + \frac{\pi}{\delta}, \theta_2 + \frac{\pi}{\delta})^{2,2}_{4,2} \pm i f(\theta_1 + \frac{\pi}{\delta}, \theta_2 + \frac{\pi}{\delta})^{2,3}_{4,3}.
\end{aligned} \tag{2.27}$$

All other components, for example ${}^{(j)}\langle \mathrm{vac}|\sigma^z|\theta_1, \theta_2\rangle^{(j)}_{+,-}$, are zero. Note that $\varepsilon = \pm$ labels on the form-factors (2.27) are inherited from spin labels in the principal regime but no longer have this interpretation in the disordered phase. Note also that the apparent $\frac{\pi}{\delta}$ shifts in the arguments of the functions f relative to [41] are again due to the fact that that our θ and the corresponding symbol

in [41], which we here denote ϑ, are related by $\theta = \vartheta - \frac{\pi}{\delta}$. We can remove these shifts by using the half-period property of theta functions given by Equation (A.6), from which it follows that

$$f(z_1 + \frac{\pi}{\delta}, z_2 + \frac{\pi}{\delta})^{a,b}_{c,d} = -i(-1)^{g_c}(-i)^{g_b} f(z_1, z_2)^{a,\bar{b}}_{\bar{c},d}.$$

Using this property leads to the following expressions for the two-spinon XYZ form-factors in the disordered regime:

$$\begin{aligned}
{}^{(j)}\langle \mathrm{vac}|\sigma^x|\theta_1,\theta_2\rangle^{(j)}_{\pm,\mp} &= (-1)^j f(\theta_1,\theta_2)^{4,1}_{1,1} \pm f(\theta_1,\theta_2)^{4,4}_{1,4}, \\
{}^{(j)}\langle \mathrm{vac}|\sigma^y|\theta_1,\theta_2\rangle^{(j)}_{\pm,\pm} &= -if(\theta_1,\theta_2)^{3,2}_{1,2} \pm (-1)^{j+1} if(\theta_1,\theta_2)^{3,3}_{1,3}, \\
{}^{(j)}\langle \mathrm{vac}|\sigma^z|\theta_1,\theta_2\rangle^{(j)}_{\pm,\pm} &= (-1)^{j+1} f(\theta_1,\theta_2)^{2,3}_{1,2} \mp f(\theta_1,\theta_2)^{2,2}_{1,3}.
\end{aligned} \tag{2.28}$$

2.6 Massless XXZ form factors

We now consider the disordered XYZ form factors in the $x \to 1$, r fixed, limit discussed in Section 2.4. For right-moving spinons, we identify $\theta = \beta$ and take the $p \to 0$ limit of the function $f(\beta_1,\beta_2)^{a,b}_{c,d}$. This limit is obtained from that of the theta functions and from the following limits:

$$\lim \overline{G}(\beta,p) = \widetilde{G}(\beta) := \exp\left(-\int_0^\infty \frac{dt}{t}\frac{\sinh((\xi+1)t)\,\sinh^2((1+\frac{\beta}{\pi i})t)}{\sinh(\xi t)\sinh(2t)\cosh(t)}\right), \quad \lim F_0 = 2(1+\xi^{-1})p^{\frac{\xi^2+\xi+1}{8\xi}}.$$

We find that only one of the six $f(\beta_1,\beta_2)^{a,b}_{c,d}$ appearing in (2.28), namely $f(\beta_1,\beta_2)^{2,3}_{1,2}$, is non-zero in this limit. As a result, the only non-zero, two-spinon massless XXZ form-factor is given by

$$\lim\ {}^{(j)}\langle \mathrm{vac}|\sigma^z|\beta_1,\beta_2\rangle^{(j)}_{\varepsilon_1,\varepsilon_2} = (-1)^{j+1}\delta_{\varepsilon_1,\varepsilon_2}\frac{(1+\xi^{-1})\widetilde{G}(\beta_1-\beta_2)}{2\,\sin\left(\frac{\beta_1}{2i}-\frac{\pi}{4}\right)\sin\left(\frac{\beta_2}{2i}-\frac{\pi}{4}\right)\cos\left(\frac{\beta_1-\beta_2+i\pi}{2i\xi}\right)}.$$

By an abuse of notation, we continue to use ${}^{(j)}\langle \mathrm{vac}|\sigma^z|\beta_1,\beta_2\rangle^{(j)}_{\varepsilon_1,\varepsilon_2}$ to refer to the massless XXZ limit of this form factor. With β_1, β_2 real, we have

$$F(\beta_1,\beta_2,\xi) := |{}^{(j)}\langle \mathrm{vac}|\sigma^z|\beta_1,\beta_2\rangle^{(j)}_{\varepsilon,\varepsilon}|^2 = \frac{2(1+\xi^{-1})^2 e^{-I_\xi(\frac{\beta_1-\beta_2}{2\pi})}}{\cosh(\beta_1)\cosh(\beta_2)(\cos(\frac{\pi}{\xi})+\cosh(\frac{\beta_1-\beta_2}{\xi}))}, \tag{2.29}$$

where the integral $I_\xi(z)$ is defined by

$$I_\xi(z) = \int_0^\infty \frac{dt}{t}\frac{\sinh((\xi+1)t}{\sinh(\xi t)}\frac{(\cosh(2t)\cos(4tz)-1)}{\sinh(2t)\cosh(t)}. \tag{2.30}$$

Note that the expression (2.29) is symmetric with respect to exchange of (β_1,β_2), and independent of both ε and j.

3 The Longitudinal Structure Factor

The longitudinal structure factor has already been defined by Equation (1.2). In order to be able to compute the form-factor expansion of this object we need to know the resolution of the identity in terms of a basis of states. We conjecture that

$$\mathbb{I} = \sum_{j=0,1}\sum_{n\geq 0}\sum_{\varepsilon_1,\cdots,\varepsilon_{2n}}\frac{1}{(2n)!}\int_{-\infty}^{\infty}\frac{d\beta_1}{2\pi}\cdots\int_{-\infty}^{\infty}\frac{d\beta_{2n}}{2\pi}|\beta_1,\cdots,\beta_{2n}\rangle^{(j)}_{\varepsilon_1,\cdots,\varepsilon_{2n}}\ {}^{(j)}_{\varepsilon_1,\cdots,\varepsilon_{2n}}\langle\beta_1,\cdots,\beta_{2n}|. \tag{3.1}$$

This conjecture is an analogue of the conjecture made in the antiferromagnetic regime of the XXZ model in [20]. Note however, that there is a slight but important difference to [20]. In considering XXZ single spinons in Section 2.2, we have characterised right-moving spinons as having momentum in the range $(0,\pi)$ and left-moving spinons as having momentum in the range $(-\pi,0)$. In (3.1) however, we only include even spinon states consisting of right-moving spinons. The reason for this are two-fold: firstly, that right-left moving pairs are simply absent from the Bethe Ansatz states, and secondly that a right-right pair already spans the entire $(0,2\pi)$ Brillouin zone - to include the left-left pair would be to double count. This point is discussed in some detail in [26] for the massive antiferromagnetic phase of the XXZ model. Independent numerical justification that we have made the correct choice of normalisation is given by the sum rule calculations in Section 4.

In writing (1.2) we have not specified to which vacuum we are referring. However, the result is the same whether we choose to use $|\mathrm{vac}\rangle^{(0)}$, $|\mathrm{vac}\rangle^{(1)}$ or the linear combinations $|\mathrm{vac}\rangle_{\pm}=\frac{1}{\sqrt{2}}(|\mathrm{vac}\rangle^{(0)}\pm|\mathrm{vac}\rangle^{(1)})$ considered in [41]. For notational convenience, let us specify that $|\mathrm{vac}\rangle=|\mathrm{vac}\rangle^{(0)}$. Then inserting the resolution (3.1) we have the 2-particle contribution

$$S_2^{zz}(k,\omega)=\frac{1}{8}\sum_{\varepsilon}\int_{-\infty}^{\infty}\int_{-\infty}^{\infty}\frac{d\beta_1}{2\pi}\frac{d\beta_2}{2\pi}\sum_{j\in\mathbb{Z}}e^{-i(k-K(\beta_1)-K(\beta_2))j}\int_{-\infty}^{\infty}dt e^{i(\omega-W(\beta_1)-W(\beta_2))t}\,|{}^{(0)}\langle\mathrm{vac}|\sigma^z|\beta_1,\beta_2\rangle^{(0)}_{\varepsilon,\varepsilon}|^2,$$

where the spinon momentum and energy are defined by

$$K(\beta)=2\arctan(e^{\beta}),\quad W(\beta)=\frac{v_F}{\cosh(\beta)}.$$

We then write both the j sum and w integral in terms of delta functions to give

$$S_2^{zz}(k,\omega)=\frac{1}{4}\int_{-\infty}^{\infty}\int_{-\infty}^{\infty}d\beta_1 d\beta_1\,\delta\big(k-K(\beta_1)-K(\beta_2)\big)\,\delta\big(\omega-W(\beta_1)-W(\beta_2)\big)\,F(\beta_1,\beta_2,\xi),\qquad(3.2)$$

where $F(\beta_1,\beta_2,\xi)$ is defined by (2.29).

We now recall that if we have a suitably smooth function $g:\mathbb{R}^2\to\mathbb{R}^2$ with a finite number of zeroes $(x_1^{(j)},x_2^{(j)})$ at which $\det g'(x_1^{(j)},x_2^{(j)})\neq 0$, and a function $f:\mathbb{R}^2\to\mathbb{R}$, then we have

$$\int_{-\infty}^{\infty}\int_{-\infty}^{\infty}dx_1dx_2\,f(x_1,x_2)\delta(g(x_1,x_2))=\sum_j\frac{f(x_1^{(j)},x_2^{(j)})}{|\det g'(x_1^{(j)},x_2^{(j)})|}.$$

To use this fact on (3.2), we make use of the determinant

$$\begin{vmatrix} W'(\beta_1) & W'(\beta_2)\\ K'(\beta_1) & K'(\beta_2)\end{vmatrix}=\frac{v_F(\tanh(\beta_2)-\tanh(\beta_1))}{\cosh(\beta_1)\cosh(\beta_2)}.$$

For each choice of k and ω in the two-spinon band there is a unique (up to exchange of $\tilde\beta_1$ and $\tilde\beta_2$) pair $(\tilde\beta_1,\tilde\beta_2)$ satisfying the combined conditions $k=K(\tilde\beta_1)+K(\tilde\beta_2)$ and $\omega=W(\tilde\beta_1)+W(\tilde\beta_2)$. Thus, (3.2) becomes

$$S_2^{zz}(k,\omega)=\frac{1}{2}\frac{\cosh(\tilde\beta_1)\cosh(\tilde\beta_2)F(\tilde\beta_1,\tilde\beta_2,\xi)}{v_F|\tanh(\tilde\beta_1)-\tanh(\tilde\beta_2)|}.$$

Let us denote the upper two-spinon energy threshold and and lower two-particle energy threshold by $\omega_{2,u}(k)$ and $\omega_{2,l}(k)$. They are given by the following expressions:

$$\omega_{2,u}(k)=2v_F\sin(k/2),\quad \omega_{2,l}(k)=v_F|\sin(k)|,\qquad(3.3)$$

where the Fermi velocity v_F is given by Equation (2.24). There is a useful identity

$$\sqrt{\omega_{2,u}^2(k) - \omega^2} = v_F |\tanh(\tilde{\beta}_1) - \tanh(\tilde{\beta}_2)|.$$

Using this identify, and substituting the expression (2.29) for the modulus squared of the form-factor, we arrive at the expression

$$S_2^{zz}(k,\omega) = \frac{\Theta(\omega_{2,u}(k) - \omega)\Theta(\omega - \omega_{2,l}(k))(1+\xi^{-1})^2 e^{-I_\xi(\frac{\beta}{2\pi})}}{\sqrt{\omega_{2,u}^2(k) - \omega^2}\,\left(\cos(\frac{\pi}{\xi}) + \cosh(\frac{\beta}{\xi})\right)}, \tag{3.4}$$

where $\beta := \tilde{\beta}_1 - \tilde{\beta}_2$ and $k = K(\tilde{\beta}_1) + K(\tilde{\beta}_2)$, $\omega = W(\tilde{\beta}_1) + W(\tilde{\beta}_2)$.

4 Results

In this section, we offer quantitative results and plots for the longitudinal structure factor (LSF). Here, for convenience of comparison with previous results in the literature, we use a slightly different convention for the Hamiltonian (corresponding to the ones we used in [15]), writing it as

$$H = J \sum_{i\in\mathbb{Z}} \left(S_i^x S_{i+1}^x + S_i^y S_{i+1}^y + \Delta S_i^z S_{i+1}^z\right) \tag{4.1}$$

where $S_i^\alpha = \frac{1}{2}\sigma_i^\alpha$, $J > 0$. We have a gauge equivalence $H = OH_{XXZ}O^\dagger$, where $O = \cdots \otimes 1 \otimes \sigma^z \otimes 1 \otimes \sigma^z \otimes \cdots$. The two-spinon part of the LSF is given by Equation (3.4) in which the parameter $\beta(k,\omega) =: 2\pi\rho(k,\omega)$ is obtained from the constraint

$$\cosh(\pi\rho(k,\omega)) = \sqrt{\frac{\omega_{2,u}^2(k) - \omega_{2,l}^2(k)}{\omega^2 - \omega_{2,l}^2(k)}}. \tag{4.2}$$

4.1 Full Brillouin zone

In Figures 1 and 2, we present plots of the two-spinon longitudinal structure factor for different values of anisotropy, starting at the XX limit and going up to the isotropic antiferromagnetic point $\Delta = 1$. All plots cover a full Brillouin zone and clearly show the continuum over which the two-spinon correlation is non-vanishing. This continuum in the k-ω plane is located between the lower and upper boundaries (3.3). In fact, for zero magnetic field, the full LSF vanishes beneath the lower boundary, i.e., for $\omega < \omega_{2,l}(k)$. All $2, 4, 6, ...$ spinon states share the line $\omega = \omega_{2,l}(k)$ as their lower boundary, and the LSF is strictly positive for all $\omega > \omega_{2,l}(k)$. Above the upper two-spinon boundary $\omega > \omega_{2,u}(k)$, the two-spinon contribution of course vanishes, but higher-spinon states can contribute.

Starting at small Δ, the top left panel of Figure 1 clearly illustrates the fact that the LSF diverges at the upper boundary (we will quantify all threshold behaviour in Section 4.5), and tends to a constant at the lower one. This is easily understood [46, 47] by mapping to a system of free fermions using the Jordan-Wigner transformation, under which the S^z operator becomes a fermionic density operator. Since the fermionic density operator in Fourier space takes the form of a convolution product of creation-annihilation operators, $\rho_k = \sum_q \psi_{k+q}^\dagger \psi_k$, and since the ground state is a simple Fermi sea of the Jordan-Wigner fermions, all form factors of the S^z operator are energy independent, and vanish for all but the two-spinon states. The LSF is thus simply a representation of the two-spinon density

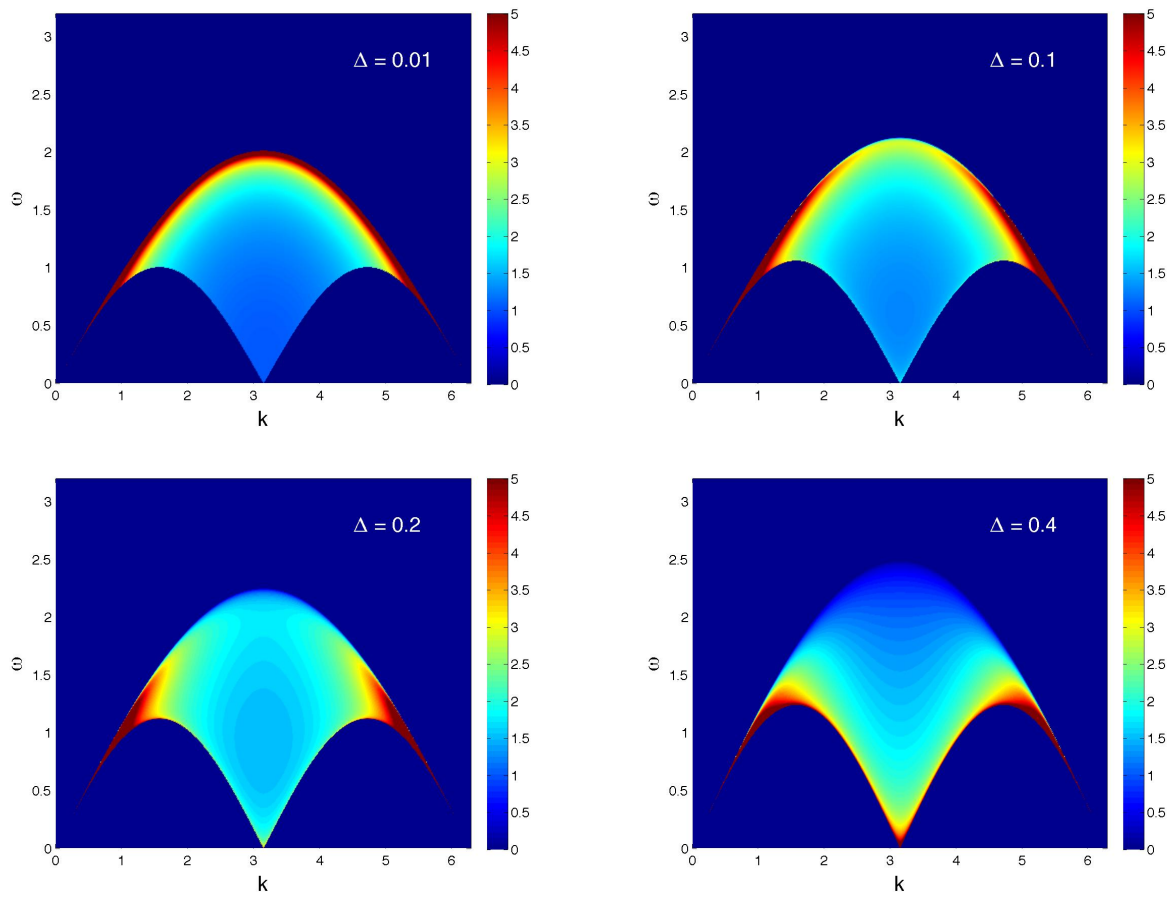

Figure 1: Two-spinon part of the longitudinal structure factor of the infinite Heisenberg chain, for different values of the anisotropy parameter Δ (see also Figure 2). For $\Delta \to 0$, the correlation follows the density of states, and has a square root singularity at the upper threshold for all values of momenta.

of states, which has a square-root divergence at the upper threshold (see, e.g., [48] for details) and is constant at the lower one.

Turning the anisotropy up leads rapidly to the loss of the divergence at the upper threshold, starting from the region $k \simeq \pi$, as can be seen in the top right panel of Figure 1. The presence of a finite Δ is most importantly felt in the form factors: while the density of states still diverges, the form factors now decrease sufficiently rapidly to kill off this divergence. Once Δ has attained values of around 0.4, the remains of the divergence at the upper threshold have been completely erased for all values of momentum away from the zone boundary, and the lower threshold starts to feel the effects of the antiferromagnetic correlations, the peak at $k = \pi$, $\omega = 0$ starting to develop.

As Δ is increased further (see Figure 2, the cascade of correlation weight towards the low-energy sector continues until the isotropic limit is attained, at which point which most of the signal is concentrated in the immediate vicinity of the lower threshold.

Throughout this series of plots (which are presented in a uniform ω and intensity scale for convenience of comparison), the slow increase of the Fermi velocity and of the reach of the two-spinon continuum can be seen.

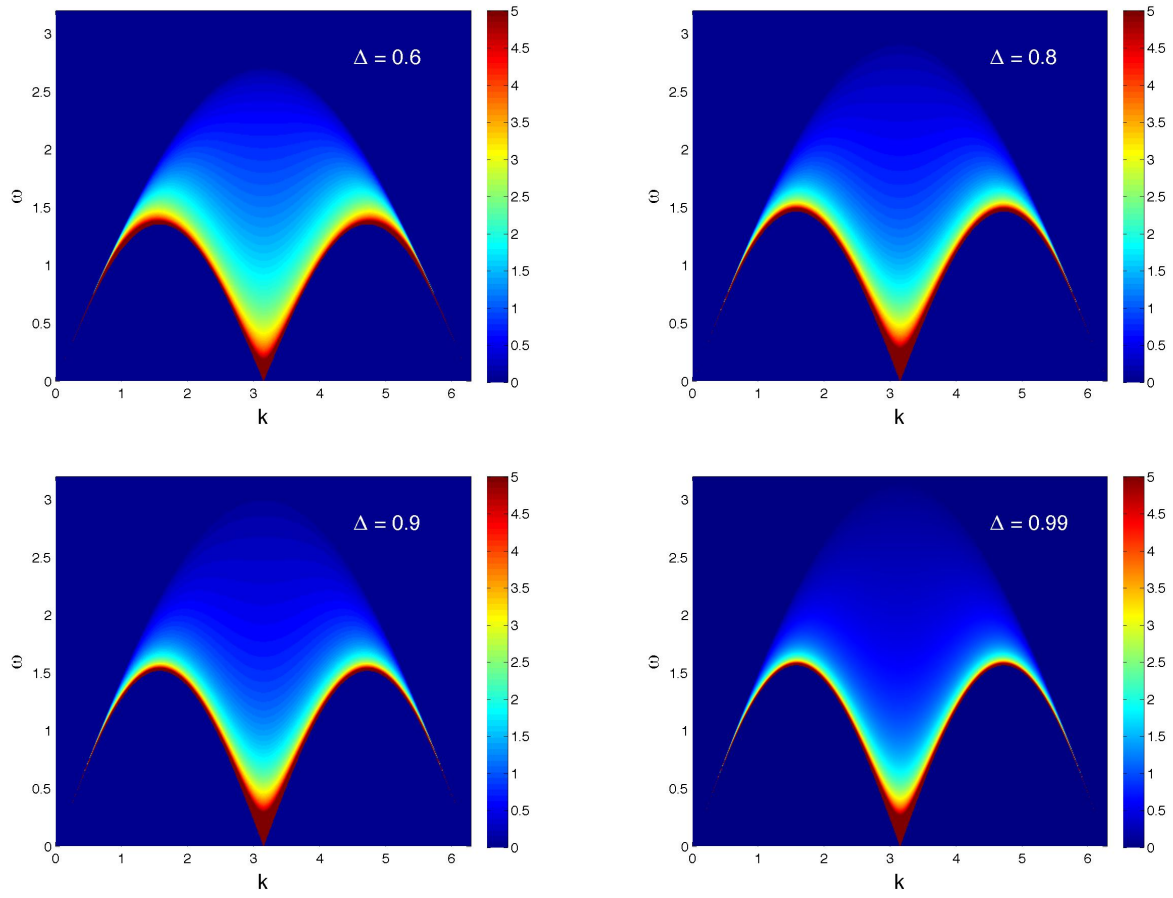

Figure 2: Two-spinon part of the longitudinal structure factor of the infinite Heisenberg chain, for different values of the anisotropy parameter Δ (see also Figure 2). Increasing the anisotropy shifts the weight progressively towards the lower boundary. The lower boundary becomes increasingly sharp as the $\Delta \to 1$ limit is approached.

4.2 Fixed momentum

In Figures 3 - 6, we provide a number of fixed-momentum cuts of the two-spinon part of the longitudinal structure factor. We organise the plots in each figure by increasing anisotropy at fixed momentum. Each individual plot also gives the $\Delta = 0$ and $\Delta = 1$ curves as a reference; the effects of tuning the anisotropy continuously between these two values can thus be easily visualised.

At $k = \pi/4$, as shown in Figure 3, the two-spinon continuum is quite narrow but its position is steadily increasing in energy as the anisotropy is turned up, since the Fermi velocity v_F (2.24) is steadily increasing with increasing anisotropy. The upper-threshold singularity at $\Delta = 0$ disappears quickly as a function of Δ, being replaced by a square-root cusp (see the discussion in Section 4.5). The singularity at the lower threshold appears immediately but takes on a significant weight only for around $\Delta \sim 0.3$ and above. The picture is very similar for the other momenta presented, namely $k = \pi/2$ (Figure 4), $k = 3\pi/4$ (Figure 5) and π (Figure 6).

4.3 Sum rules

The full Hilbert space of the model in the zero magnetisation sector contains many more states than the simple two-spinon states we have considered. Two-spinon states in fact represent only a vanishingly small fraction of the total number of states when the system size goes to infinity. It is thus a remarkable fact that these simple states can carry a non-vanishing fraction of any correlation function.

To quantify the importance of the two-spinon contribution to the longitudinal structure factor, we consider two sum rules. First of all, we use the integrated intensity

$$I^{zz} = \int_0^{2\pi} \frac{dk}{2\pi} \int_0^{\infty} \frac{d\omega}{2\pi} S(k,\omega) = \frac{1}{4}, \tag{4.3}$$

obtained from the simple real space-time correlator $\langle S^z_{j'=j}(t=0) S^z_j(0)\rangle = \frac{1}{4}$. A less trivial sum rule comes from considering the integrated first frequency moment of the structure factor, giving the so-called f-sumrule (at fixed momentum) [49],

$$I_1^{zz}(k) = \int_0^{2\pi} \frac{d\omega}{2\pi} \omega S(k,\omega) = -\frac{1}{2} \langle \left[\left[H, S^z_q \right], S^z_{-q} \right] \rangle = -2X^x(1-\cos k), \tag{4.4}$$

where $S^z_q := \frac{1}{\sqrt{N}} \sum_j e^{iqj} S^z_j$ is the Fourier transform of the local magnetisation operator and $X^x := \langle S^x_j S^x_{j+1} \rangle$ is the ground state expectation value of the in-plane exchange term. The explicit value of the right-hand side of this identity can be obtained from the ground-state energy density e_0 [50] and its derivative using the Feynman-Hellman theorem, namely $X^x = \frac{1}{2J}(1 - \Delta \frac{\partial}{\partial \Delta}) e_0$, with

$$e_0 = \frac{-J(\xi+1)}{2\pi} \sin\left[\frac{\pi}{\xi+1}\right] \int_{-\infty}^{\infty} dt \left(1 - \frac{\tanh t}{\tanh[(\xi+1)t]}\right). \tag{4.5}$$

The level of saturation of the two sum rules coming from two-spinon intermediate states is inevitably anisotropy dependent. We provide the explicit values of the sum rule saturations coming from two-spinon contributions in Table 2 (for the f-sumrule, the saturation turns out to be exactly the same at all momenta). Two-spinon states carry the totality of the correlation at $\Delta = 0$, a result which can be understood by considering the mapping to free fermions using the Jordan-Wigner transformation mentioned previously. Two-spinon states are the only intermediate states contributing to

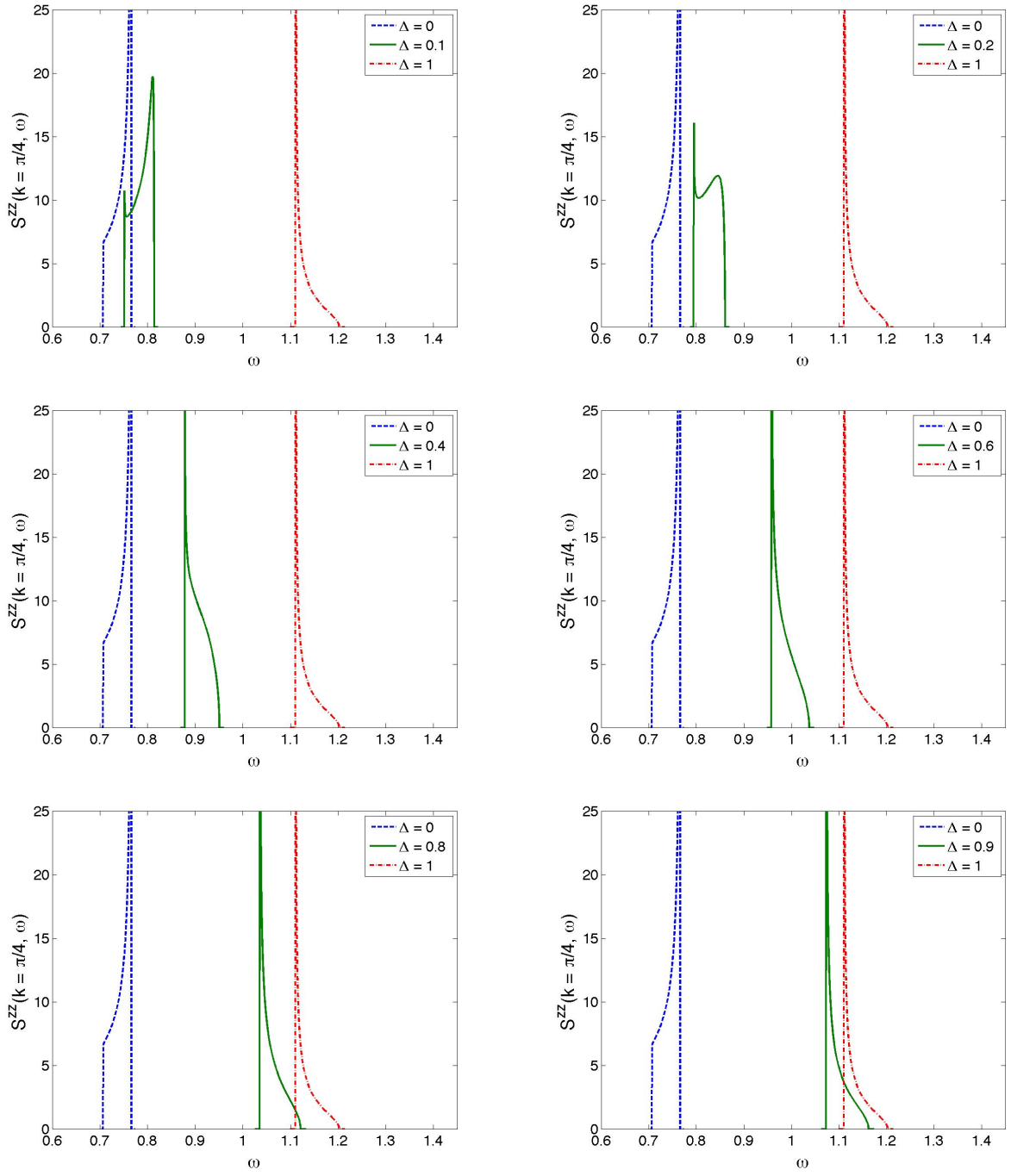

Figure 3: Fixed momentum cuts at $k = \pi/4$ of the two-spinon part of the longitudinal structure factor of the infinite Heisenberg chain, for different values of the anisotropy parameter Δ. The $\Delta = 0$ and $\Delta = 1$ limits are displayed in all plots for comparison.

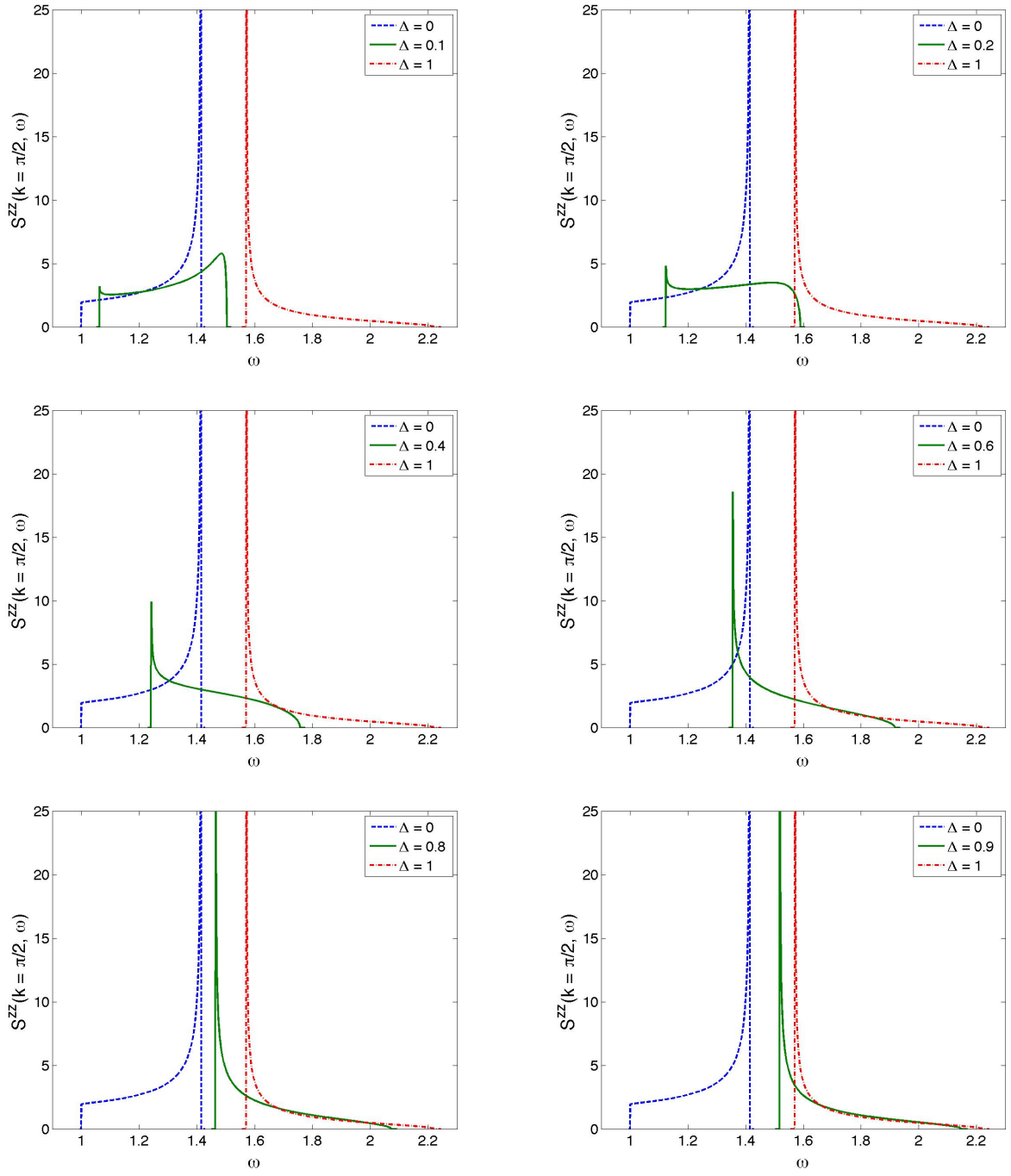

Figure 4: Fixed momentum cuts at $k = \pi/2$ of the two-spinon part of the longitudinal structure factor of the infinite Heisenberg chain, for different values of the anisotropy parameter Δ. The $\Delta = 0$ and $\Delta = 1$ limits are displayed in all plots for comparison.

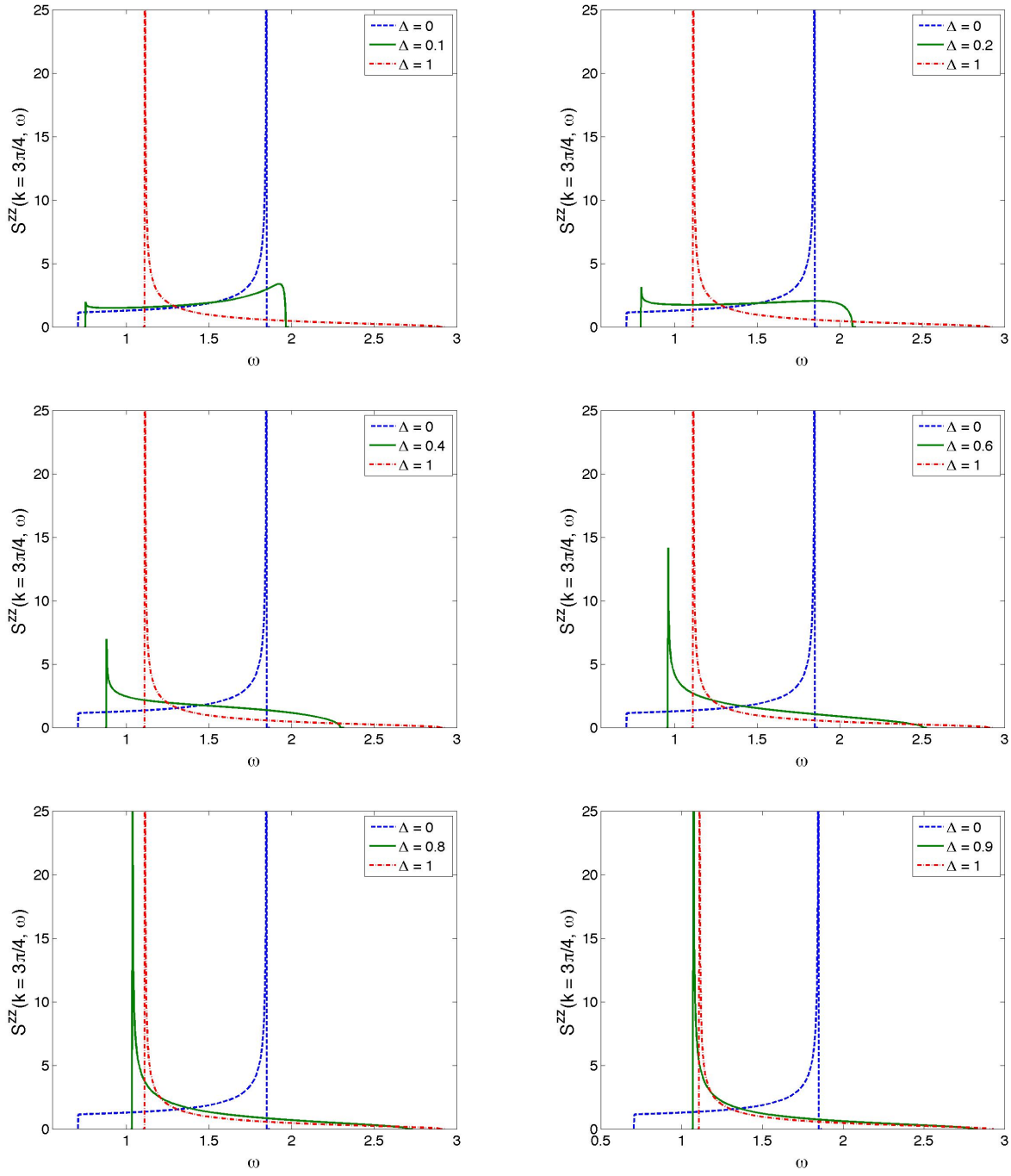

Figure 5: Fixed momentum cuts at $k = 3\pi/4$ of the two-spinon part of the longitudinal structure factor of the infinite Heisenberg chain, for different values of the anisotropy parameter Δ. The $\Delta = 0$ and $\Delta = 1$ limits are displayed in all plots for comparison.

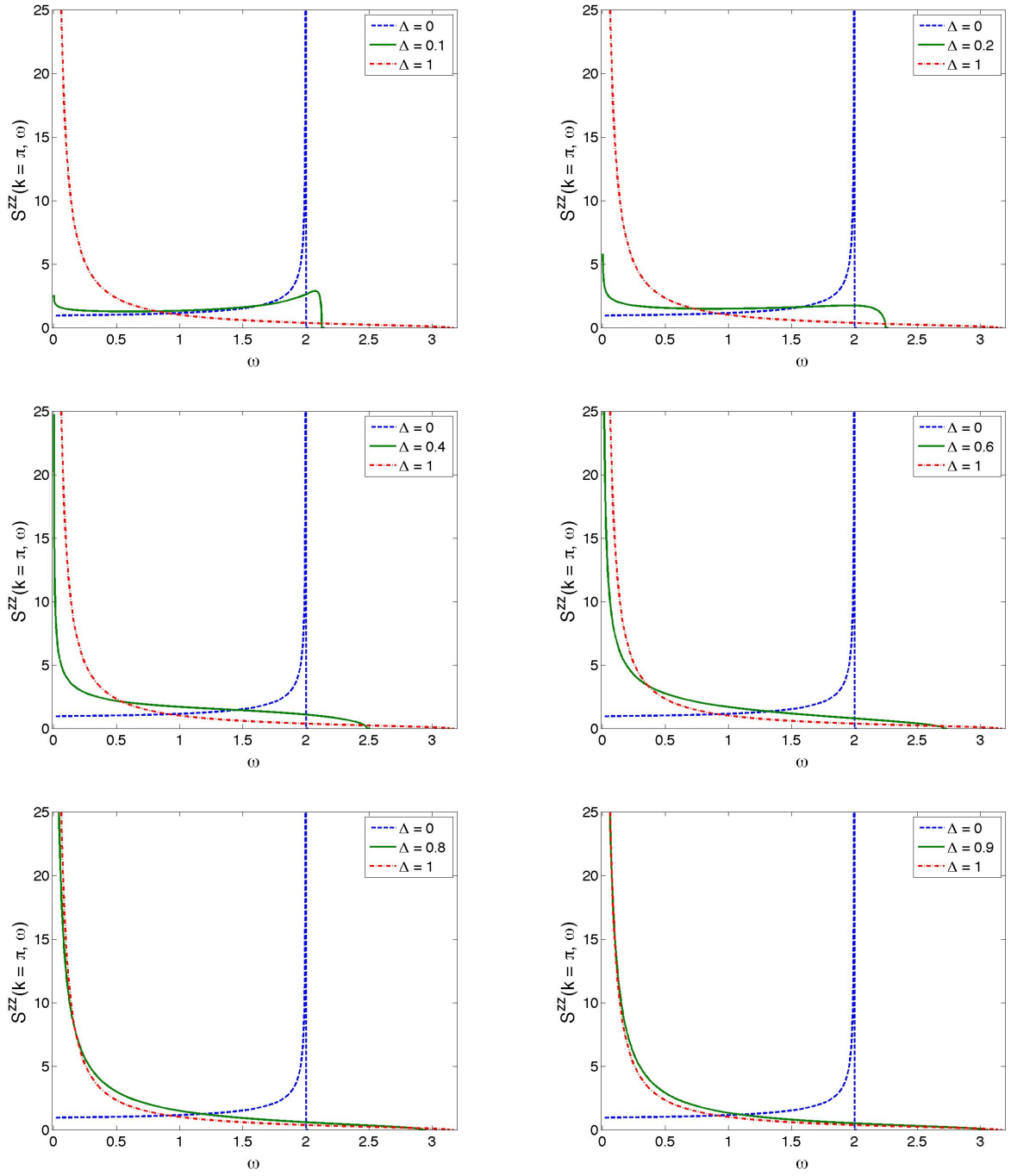

Figure 6: Fixed momentum cuts at $k = \pi$ of the two-spinon part of the longitudinal structure factor of the infinite Heisenberg chain, for different values of the anisotropy parameter Δ. The $\Delta = 0$ and $\Delta = 1$ limits are displayed in all plots for comparison.

the longitudinal structure factor, and the sum rules are saturated to 100%. Our results are of course consistent with this fact.

A more remarkable fact is that the subset of two-spinon states continues to play such a determinantal role in carrying the longitudinal structure factor even when the anisotropy has been turned on to significant values. As our results show, two-spinon states carry essentially all the correlation weight up to surprisingly large values of interactions $\Delta \sim 0.8$, above which four, six, ... spinon states become harder to neglect. This is quite surprising since, reasoning again in the fermionic language obtained from the Jordan-Wigner transformation, the interaction should be able to create multiple particle-hole states quite easily, and arbitrarily complicated higher-spinon states should therefore participate in the correlation, leaving two-spinon states only negligible contribution. While true in the generic finite magnetic field case, it turns out that for zero magnetic field, the available particle phase-space shrinks to zero, and only the hole (spinon) part can disperse. The longitudinal structure factor thus possesses a finite two-spinon contribution, which is not true for example of the transverse structure factor.

Δ	I^{zz}_{2sp}/I^{zz}	$I^{zz}_{1,2sp}/I^{zz}_1$		Δ	I^{zz}_{2sp}/I^{zz}	$I^{zz}_{1,2sp}/I^{zz}_1$
0	1	1		0.6	0.9778	0.9743
0.1	0.9997	0.9997		0.7	0.9637	0.9578
0.2	0.9986	0.9984		0.8	0.9406	0.9314
0.3	0.9964	0.9959		0.9	0.8980	0.8844
0.4	0.9927	0.9917		0.99	0.7918	0.7748
0.5	0.9869	0.9849		0.999	0.7494	0.7331

Table 2: Sum rule saturations as a function of anisotropy: two-spinon contribution to the integrated intensity I^{zz} (4.3) and first frequency moment I^{zz}_1 (4.4).

4.4 Correspondence with finite size results

The longitudinal structure factor can also be obtained at finite size using explicit summations over intermediate states, as performed in [51, 52]. At finite size (i.e., when the chain is made of N sites; we take N even to ensure a non-degenerate ground state at zero field), two-spinon states in zero field are those eigenstates obtained using $N/2-1$ real rapidities and a single negative-parity one-string (those readers unfamiliar with this nomenclature are referred to the explanations in [52]). The total number of such states then corresponds to the number of ways of choosing two hole quantum numbers from $N/2+1$ available ones, and thus equals $N(N+2)/8$. We can thus, at a fixed size N, sum over the contributions to (1.2) coming from these two-spinon states, and compare with our infinite-size result.

Figure 7 presents such a comparison, done at a representative value of anisotropy $\Delta = 0.7$ and two values of momentum, $k = \pi/2$ and $k = \pi$. Other values of anisotropy and momenta give qualitatively similar plots. Besides the thermodynamic limit curve obtained from plotting the two-spinon contribution we have obtained, we also present the equivalent curves for three different system sizes, $N = 256, 512$ and 1024. The finite-size results must be smoothed with a gaussian, since the correlation function is then a sum of delta-function peaks split in energy by the mean energy level spacing. This smoothing can be sharpened at increasing system size, and this increasing sharpness can be clearly seen, e.g., at the lower boundary of the $k = \pi/2$ plot. It is clear that the finite-size curves tend to the

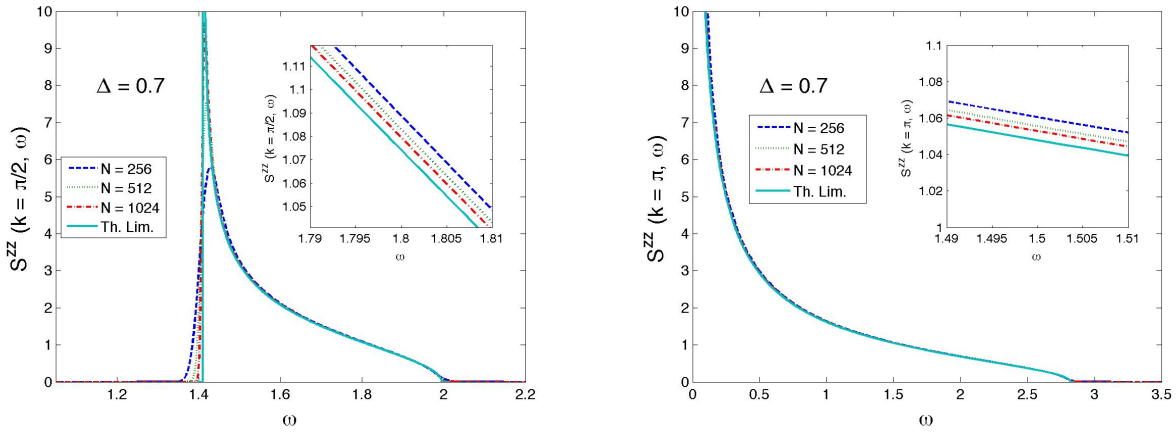

Figure 7: Comparison between the two-spinon longitudinal structure factor for $\Delta = 0.7$ and momentum $k = \pi/2$ (left) and $k = \pi$ (right), in the thermodynamic limit (solid curve) and at finite size. The finite size results are obtained by summing exactly over the set of $N(N+2)/8$ two-spinon states at chain length N, and are plotted after gaussian smoothing of the delta function contributions. See main text for more details.

thermodynamic one as system size increases; the inset of each plot offers a magnified view of a selected region away from the singular thresholds, the quantitative differences between the highest system size considered and the infinite size limit being of the order of a percent.

N	I^{zz}_{2sp}/I^{zz}	$I^{zz}_{1,2sp}(\pi/2)/I^{zz}_1$	$I^{zz}_{1,2sp}(\pi)/I^{zz}_1$
64	0.9893	0.9825	0.9852
128	0.9843	0.9778	0.9776
256	0.9796	0.9733	0.9713
512	0.9756	0.9695	0.9668
1024	0.9724	0.9664	0.9636
extrap	0.963(2)	0.957(4)	0.957(4)
∞	0.9637	0.9578	0.9578

Table 3: Sum rule contributions obtained from the finite-size calculation of the two-spinon contributions to the longitudinal structure factor at the representative value of anisotropy $\Delta = 0.7$, for system sizes up to $N = 1024$ and extrapolated (see text), as compared to the analytical result at infinite system size. See main text for more details.

In Table 3, we provide quantitative results for the sum rule contributions for the representative value of anisotropy $\Delta = 0.7$. Similarly to Table 2, we provide both the integrated intensity sum rule contribution (4.3) as well as the f-sumrule one (4.4), coming from two-spinon states. The results at finite size are clearly seen to tend to their infinite-size limit. For completeness, we have extrapolated the finite-size results using data at $N = 256, 512, 768$ and 1024, fitting with a polynomial in $1/\sqrt{N}$. Within the accuracy of the extrapolation, these results coincide with the ones obtained from the analytical form.

4.5 Threshold behaviour

The investigation of the precise form of the longitudinal structure factor near the upper and lower boundaries of the two-spinon continuum, which our results render possible, is of considerable theoretical interest in view of recent developments in the general phenomenology of one-dimensional quantum liquids [53, 54, 55] coming from efforts to calculate dynamical correlations away from the low-energy limit [56, 57, 58, 59, 60, 61, 62]. For the special case of the longitudinal structure factor of the zero-field gapless XXZ antiferromagnet we are considering, which is equivalent to the density-density correlator of spinless interacting fermions obtained via a Jordan-Wigner transformation, the field theory predictions of [61, 62] yield a singular LSF in the vicinity of the lower/upper thresholds of the two-spinon continuum. In the vicinity of the upper threshold, for $0 < \Delta < 1$, this singularity is shown to be of the form $S^{zz}(k,\omega) \xrightarrow[\omega\to\omega_{2,u}(k)]{} \sqrt{\omega_{2,u}(k)-\omega}$. For the lower threshold, the power-law becomes anisotropy-dependent, $S^{zz}(k,\omega) \xrightarrow[\omega\to\omega_{2,l}(k)]{} (\omega-\omega_{2,l}(k))^{-(1-K)}$ in which K is the Luttinger parameter, which for the zero field XXZ model takes the value $K = \frac{1}{2}(1-\frac{\mathrm{acos}\Delta}{\pi})^{-1}$. In terms of the parameter ξ, the Luttinger parameter becomes $K = \frac{1}{2}(1+\frac{1}{\xi})$. Our discussion here has two aims: firstly, to reproduce and possibly refine the determination of this threshold behaviour; secondly, to quantify its region of validity, which is very difficult to achieve within nonlinear Luttinger liquid theory.

Let us thus consider evaluating the two-spinon part of the longitudinal structure factor in the vicinity of the excitation thresholds, starting from our exact representation (3.4). We consider the explicit evaluation of the fundamental integral (2.30) in various limits. For convenience, we rewrite it as

$$I_\xi(\rho) = I_\xi^{(1)}(\rho) - I_\xi^{(2)}(\rho),$$

where

$$I_\xi^{(1)}(\rho) := \int_0^\infty \frac{dt}{t}\frac{\sinh(\xi+1)t}{\sinh\xi t}\frac{\sinh t}{\cosh^2 t}\cos 4\rho t, \tag{4.6}$$

$$\text{and } I_\xi^{(2)}(\rho) := \int_0^\infty \frac{dt}{t}\frac{\sinh(\xi+1)t}{\sinh\xi t}\frac{\sin^2 2\rho t}{\sinh t\cosh^2 t}. \tag{4.7}$$

Throughout the discussion below, unless we specifically mention otherwise, we consider the generic case $\xi = \mathrm{O}(1)$.

4.5.1 The structure factor near the upper threshold.

In order to obtain the structure factor near the upper boundary of the two-spinon continuum, i.e., $\omega \to \omega_{2,u}(k)$, we must consider the limit $\rho \to 0$ of the fundamental integral. Let us thus look at the two integrals (4.6) and (4.7) in turn.

a) $I_\xi^{(1)}(\rho)$**:** For $\rho = 0$, the integrand of $I^{(1)}$ is regular at $t \to 0$, but the integral diverges logarithmically as $t \to \infty$. We thus expect a log divergence as a function of ρ, $I_\xi^{(1)}(\rho) \to -c\ln\rho + d$ where $c > 0$ and $c, d = \mathrm{O}(1)$. We can in fact immediately predict the value of the coefficient c by looking at the ratio of hyperbolic functions, which tends to 2 at $t \to \infty$, so $c = 2$. This is easily proved by rewriting $I_\xi^{(1)}$ (defining $f_\xi^{(1)}(t) := \frac{\sinh(\xi+1)t}{\sinh\xi t}\frac{\sinh t}{\cosh^2 t}$) using the cosine integral Ci as

$$I_\xi^{(1)}(\rho) = I_\xi^{(11)}(\rho|\bar{t}_1) + I_\xi^{(12)}(\rho|\bar{t}_1) - 2\mathrm{Ci}(4\rho\bar{t}_1),$$

in which $\bar{t}_1$ is an arbitrary real number and

$$I_\xi^{(11)}(\rho|\bar{t}_1) := \int_0^{\bar{t}_1} \frac{dt}{t} f_\xi^{(1)}(t) \cos 4\rho t, \quad I_\xi^{(12)}(\rho|\bar{t}_1) := \int_{\bar{t}_1}^{\infty} \frac{dt}{t} (f_\xi^{(1)}(t) - 2) \cos 4\rho t,$$

and we have used the identity

$$\int_{\bar{t}_1}^{\infty} \frac{dt}{t} \cos 4\rho t = -\mathrm{Ci}(4\rho \bar{t}_1).$$

Let us choose $\bar{t}_1 = \mathrm{O}(1)$. We then have

$$|I_\xi^{(11)}(\rho)| \leq \int_0^{\bar{t}_1} \frac{dt}{t} f_\xi^{(1)}(t) = \mathrm{O}(1).$$

We thus have explicit convergence of the first integral, $\lim_{\rho\to 0} I_\xi^{(11)}(\rho|\bar{t}_1) = \mathrm{O}(1)$.

$I^{(12)}$ also converges explicitly for generic $\xi = \mathrm{O}(1)$,

$$|I_\xi^{(11)}(\rho)| \leq \int_{\bar{t}_1}^{\infty} \frac{dt}{t} |(f_\xi^{(1)}(t) - 2)| = \mathrm{O}(1).$$

The only problematic terms as $\rho \to 0$ are therefore relegated to the cosine integral, which can be rewritten to separate out the singular ρ dependence,

$$\mathrm{Ci}(4\rho\bar{t}) = \mathbf{C} + \ln\rho + \ln(4\bar{t}) - 2\int_0^{\bar{t}} \frac{dt}{t} \sin^2 2\rho t.$$

We thus obtain the partial result

$$I_\xi^{(1)}(\rho) \xrightarrow[\rho\to 0]{} -2\ln\rho + \mathrm{O}(1).$$

b) $I_\xi^{(2)}(\rho)$**:** The integrand of $I^{(2)}$ vanishes sufficiently rapidly at $t \to 0$ and $t \to \infty$, so this integral yields a contribution of order $\rho^2 \to 0$. Thus no nontrivial contribution to the structure factor comes from this integral in the limit considered.

This means that overall, we have

$$I_\xi(\rho) \xrightarrow[\rho\to 0]{} -2\ln\rho + \mathrm{O}(1). \tag{4.8}$$

We thus have (using $\rho \sim \sqrt{\omega_{2,u}(k) - \omega}$ from (4.2))

$$S_2^{zz}(k,\omega) \xrightarrow[\omega\to\omega_{2,u}(k)]{} f_u(\xi)(\sin\frac{k}{2})^{-7/2}\sqrt{\omega_{2,u}(k) - \omega} \tag{4.9}$$

in which $f_u(\xi)$ is a momentum-independent function of anisotropy. The exponent we obtain confirms the field theory predictions [61] for the anisotropy-independent square-root cusp at the threshold (for $0 < \Delta \leq 1$). Our results allow us additionally to extract a strongly momentum-dependent prefactor, which greatly enhances the spectral weight around the zone boundaries at $k = 0, 2\pi$, as is also noticeable in the figures.

For the $\Delta \to 0$ limit (so $\xi \to 1$), we have to take the limit more carefully, since the $\cosh \frac{2\pi\rho}{\xi} + \cos\frac{\pi}{\xi}$ in the denominator of the structure factor now vanishes when $\rho \to 0$. Overall, in this case one rather obtains a square-root divergence,

$$S_2^{zz}(k,\omega) \xrightarrow[\omega\to\omega_{2,u}(k)]{} f_u(1)\frac{(\sin\frac{k}{2})^{-1/2}}{\sqrt{\omega_{2,u}(k)-\omega}} \tag{4.10}$$

as expected, since in this non-interacting case the structure factor simply follows the density of two-spinon states, all two-spinon form factors being energy independent and equal to each other.

4.5.2 The structure factor near the lower threshold

To evaluate the structure factor near the lower threshold of the two-spinon continuum, i.e., for $\omega \to \omega_{2,l}(k)$, we need to consider the limit $\rho \to \infty$ of the fundamental integral. Here, we again consider $\xi = \mathrm{O}(1)$, and split the integrals precisely as before, using (4.6), (4.7). Again choosing $\bar{t}_1 = \mathrm{O}(1)$, we can see that $I_\xi^{(11)}(\rho)$ is still bounded by a constant, and so is $I_\xi^{(12)}(\rho)$. In fact, since the integrands oscillate rapidly, this constant is zero. Moreover, the cosine integral evaluated at infinity also vanishes, so we have $I_\xi^{(1)}(\rho) \xrightarrow[\rho\to\infty]{} 0$.

For $I_\xi^{(2)}(\rho)$, we start by writing

$$I_\xi^{(2)}(\rho) = I_\xi^{(21)}(\rho) + I_\xi^{(22)}(\rho), \tag{4.11}$$

where we have defined

$$I_\xi^{(21)}(\rho) = \int_0^\infty \frac{dt}{t}\frac{2\sin^2 2\rho t}{\sinh 2t}, \qquad I_\xi^{(22)}(\rho) = \int_0^\infty \frac{dt}{t}\frac{\sin^2 2\rho t}{\tanh\xi t\cosh^2 t}. \tag{4.12}$$

We have

$$I_\xi^{(21)}(\rho) = \ln\cosh\pi\rho \simeq \pi\rho + \mathrm{O}(1). \tag{4.13}$$

We can evaluate $I_\xi^{(22)}(\rho)$ for large ρ by splitting it up,

$$I_\xi^{(22)}(\rho) = \int_0^{\bar{t}_2} \frac{dt}{t}\frac{\sin^2 2\rho t}{\tanh\xi t\cosh^2 t} + \int_{\bar{t}_2}^\infty \frac{dt}{t}\frac{\sin^2 2\rho t}{\tanh\xi t\cosh^2 t} \tag{4.14}$$

Let us choose $\bar{t}_2 = 1/\sqrt{\rho}$ (any power between 0 and 1 would do). For the first integral, we can write

$$\int_0^{1/\sqrt{\rho}} \frac{dt}{t}\frac{\sin^2 2\rho t}{\tanh\xi t\cosh^2 t} = \frac{2\rho}{\xi}(1+\mathrm{O}(\rho^{-2}))\int_0^{2\sqrt{\rho}} dt\frac{\sin^2 t}{t^2}. \tag{4.15}$$

We also have

$$\int_0^{2\sqrt{\rho}} dt\frac{\sin^2 t}{t^2} = \frac{\pi}{2} - \frac{1}{4}\frac{1}{\sqrt{\rho}} + \mathrm{O}(1/\rho). \tag{4.16}$$

In the second integral (from $\bar{t}_2 = 1/\sqrt{\rho}$ to ∞), $\sin^2 2\rho t$ rapidly oscillates and we can thus replace it by $1/2$ when taking the limit $\rho \to \infty$. This yields

$$\int_{1/\sqrt{\rho}}^\infty \frac{dt}{t}\frac{\sin^2 2\rho t}{\tanh\xi t\cosh^2 t} = (1+\mathrm{O}(\rho^{-1}))\frac{1}{2}\int_{1/\sqrt{\rho}}^\infty \frac{dt}{t}\frac{1}{\tanh\xi t\cosh^2 t}$$

$$= (1+\mathrm{O}(\rho^{-1}))\left[\frac{1}{2}\int_{1/\sqrt{\rho}}^\infty \frac{dt}{t}\left(\frac{1}{\tanh\xi t\cosh^2 t} - \frac{1}{\xi t}\right) + \frac{\sqrt{\rho}}{2\xi}\right] = \frac{\sqrt{\rho}}{2\xi} + \mathrm{O}(1).$$

Adding up, we thus get

$$I_\xi^{(2)}(\rho) \xrightarrow[\rho\to\infty]{} \pi\left(1+\frac{1}{\xi}\right)\rho + \mathrm{O}(1).$$

This means that the overall behaviour of the fundamental integral is

$$I_\xi(\rho) \xrightarrow[\rho\to\infty]{} -\pi\left(1+\frac{1}{\xi}\right)\rho + \mathrm{O}(1). \tag{4.17}$$

We thus find (using $\rho \sim \frac{1}{2\pi}\ln(\frac{1}{\omega-\omega_{2,l}(k)})$ from (4.2)) that the structure factor behaves as

$$S_2^{zz}(k,\omega) \xrightarrow[\omega\to\omega_{2,l}(k)]{} f_l(\xi)\frac{|\sin k|^{-\frac{1}{2}(1-\frac{1}{\xi})}(\sin\frac{k}{2})^{-\frac{2}{\xi}}}{[\omega-\omega_{2,l}(k)]^{\frac{1}{2}(1-\frac{1}{\xi})}}, \tag{4.18}$$

where $f_l(\xi)$ is again a momentum-independent function of anisotropy. This result assumes that $k \neq \pi$; at the antiferromagnetic point $k=\pi$, the behaviour becomes $1/\omega^{1-\frac{1}{\xi}}$ due to the vanishing of $\omega_{2,l}$.

For the $\Delta \to 0$ limit (so $\xi \to 1$), we thus get

$$S_2^{zz}(k,\omega) \xrightarrow[w_{\omega\to\omega_{2,l}(k)}]{} cst, \qquad \Delta = 0 \tag{4.19}$$

as expected, since the two-spinon density of states is simply a constant in this region of the continuum, and so are the form factors.

Our analytical form for the two-spinon part of the structure factor has thus allowed us to reobtain the threshold exponents predicted from field theory, and to complement the threshold behaviour of the longitudinal structure factor with momentum-dependent prefactors hard to access within that method.

One final comment here concerns the potential effect of higher-spinon states on the threshold behaviour. For the generic $0 < \Delta < 1$ case, the obtained threshold exponents would remain unchanged upon the addition of these contributions, since the power series in the energy distance $\delta\omega$ to the singularity cannot contain any logarithmic terms which could re-exponentiate into a different power law. The prefactor might however be corrected.

4.5.3 Region of validity of threshold behaviour

We now compare the behaviour at the lower and upper thresholds with the numerical evaluation of expression (3.4) in order to see over what range of frequencies these threshold formulae are valid. We do this in two different ways. The first way consists in evaluating the ratio S_2^{zz}/S_{thr}^{zz} at fixed momentum as a function of ω, in which S_{thr}^{zz} represents the relevant threshold behaviour in equations (4.9,4.18) (the prefactors $f_{u,l}(\xi)$ being obtained numerically directly from the exact representation (3.4)), and to find the region of ω near the singularity for which this ratio remains one within the required accuracy. The second way consists in actually fitting a plot of the exact expression (3.4) with the expected threshold power law over a finite but small frequency region near the singularity, and to then check over which interval in frequency this fit remains consistent. The latter method emulates the kind of fitting one might do starting from approximate ab-initio numerical data for the structure factor, and gives an overestimate of the region of validity. The two methods give results consistent

with each other when the region of validity is at least of a few percent of the available continuum. Otherwise the stricter first way gives a much smaller region of validity.

Tables 4 , 5 and 6 summarise where the difference between the threshold formula and the numerics becomes more than 1% and 10%, as a percentage of the numerical result, using the first criterion. The entries in the final four columns of these tables show the approximate percentage of the ω range $(\omega_u - \omega_l)$ that the threshold behaviour is valid for (within 1% and 10%). For example, for $\Delta = 0.5$ and $k = 0.125$ (the first row in Table 5), the formula for the upper threshold is within 1% of the result for $\sim 7\%$ of the ω range, and within 10% of the result for $\sim 47\%$ of the ω range.

It is immediately obvious that the region of validity of the lower and upper threshold behaviours depends strongly on the anisotropy. For low anisotropy, the upper threshold is not fitted well, the lower one being better described. For intermediate anisotropy the fitting is very reasonable, and covers a substantial range (over half) of the continuum. At high anisotropy, the lower threshold is not well fitted, whereas the upper one is rather well approximated. One point to notice is that the range of correspondence between the lower threshold behaviour and the exact structure factor for momenta at or near π is very narrow: in this case, subleading terms correcting the theshold behaviour should not be neglected (the very low percentages presented in some entries in the tables should however be considered as indicative only, in view of numerical difficulties in evaluating the structure factor in the immediate vicinity of thresholds). On the other hand, the less sensitive second way of fitting gives acceptable fits over a wider range of frequencies. Plots for the structure factor accompanied by the threshold fits using this second way are given for these three values of anisotropy and momentum values in Figures 8-10.

$k/(2\pi)$	w_l	w_u	Lower $< 1\%$	Lower $< 10\%$	Upper $< 1\%$	Upper $< 10\%$
0.125	0.751	0.813	$\sim 1\%$	$\sim 12\%$	$< 0.1\%$	$\sim 0.6\%$
0.25	1.06	1.50	$\sim 1.2\%$	$\sim 14\%$	$< 0.1\%$	$\sim 0.5\%$
0.375	0.751	1.96	$\sim 1.8\%$	$\sim 20\%$	$< 0.1\%$	$\sim 0.4\%$
0.5	0	2.13	$< 0.1\%$	$\sim 0.9\%$	$< 0.1\%$	$\sim 0.3\%$

Table 4: Approximate validity of threshold results for anisotropy $\Delta = 0.1$. These results are based on the first way of fitting discussed in the text. The low percentages are very approximate.

$k/(2\pi)$	w_l	w_u	Lower $< 1\%$	Lower $< 10\%$	Upper $< 1\%$	Upper $< 10\%$
0.125	0.919	0.994	$\sim 16\%$	$\sim 38\%$	$\sim 7\%$	$\sim 47\%$
0.25	1.30	1.84	$\sim 16\%$	$\sim 38\%$	$\sim 9\%$	$\sim 52\%$
0.375	0.919	2.40	$\sim 11\%$	$\sim 35\%$	$\sim 13\%$	$\sim 57\%$
0.5	0	2.60	$< 0.1\%$	$\sim 0.1\%$	$\sim 14\%$	$\sim 50\%$

Table 5: Approximate validity of threshold results for anisotropy $\Delta = 0.5$. These results are based on the first way of fitting discussed in the text. The low percentages are very approximate.

$k/(2\pi)$	w_l	w_u	Lower $< 1\%$	Lower $< 10\%$	Upper $< 1\%$	Upper $< 10\%$
0.125	1.07	1.16	$< 0.1\%$	$\sim 0.3\%$	$\sim 1.8\%$	$\sim 16\%$
0.25	1.52	2.15	$< 0.1\%$	$\sim 0.3\%$	$\sim 1.8\%$	$\sim 16\%$
0.375	1.07	2.81	$< 0.1\%$	$\sim 0.25\%$	$\sim 1.7\%$	$\sim 14\%$
0.5	0	3.04	$< 0.1\%$	$< 0.1\%$	$\sim 1.2\%$	$\sim 11\%$

Table 6: Approximate validity of threshold results for anisotropy $\Delta = 0.9$. These results are based on the first way of fitting discussed in the text. The low percentages are very approximate.

5 Conclusion

In summary, we have presented an analytical expression for the two-spinon contribution to the longitudinal structure factor of the XXZ chain in the gapless antiferromagnetic regime $0 \leq \Delta \leq 1$ for zero field in the infinite size limit at zero temperature. Our results extend to this region previous results for the isotropic or gapped antiferromagnet.

The question of the transverse structure factor remains difficult for the methods presented here. In the basis we are using, all transverse spin operator form factors vanish upon taking the gapless limit, and this points to the need for a resummation over states including macroscopic numbers of spinons, something which goes beyond current capabilities. Extending these results to the case of a finite magnetic field faces similar issues; the restriction to zero temperature is even more severe. We leave these questions open for the moment.

Another important (but now feasible) extension to our work would be to consider higher-spinon contributions to the longitudinal structure factor. This was actually performed for the isotropic XXX antiferromagnet in the recent past [24]; one can expect that such a calculation would yield the longitudinal structure factor to around 1% accuracy for any value of anisotropy in the gapless antiferromagnetic regime in zero field. It would also allow us to further refine the determination of the threshold behaviour and of its limit of applicability. We will investigate these and other issues in the future.

Acknowledgements

J.-S. C. acknowledges support from the Foundation for Fundamental Research on Matter (FOM), which is part of the Netherlands Organisation for Scientific Research (NWO). H.K is supported by the Grant-in -Aid for Scientific Research (C) 22540022 JSPS, Japan. M. S. gratefully acknowledges support from the Australian Research Council (ARC). R. W. would like to thank Nikolai Kitanine for useful discussions.

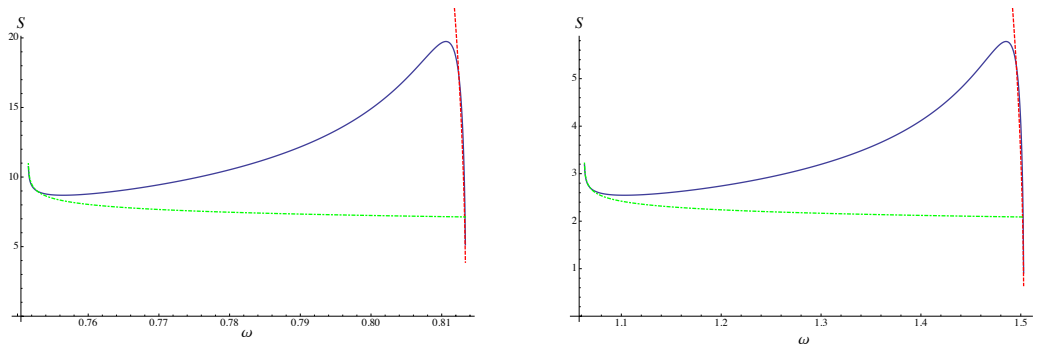

(a) $k/2\pi = 0.125$ (b) $k/2\pi = 0.25$

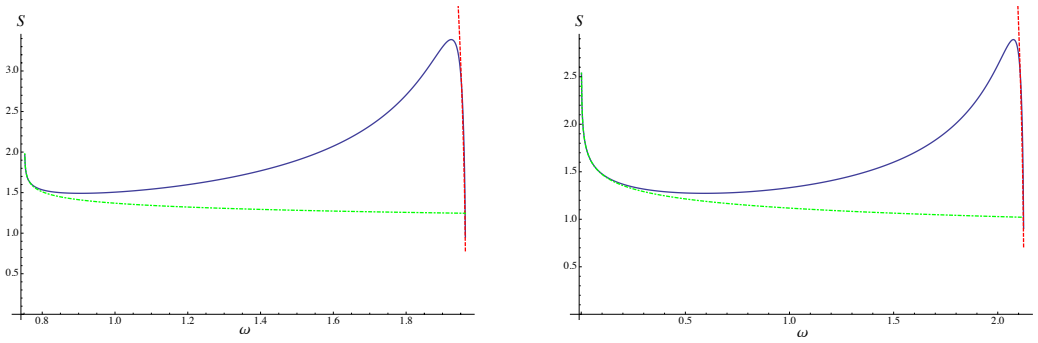

(c) $k/2\pi = 0.375$ (d) $k/2\pi = 0.5$

Figure 8: Threshold behaviour for $\Delta = 0.1$, the solid line is the numerical evaluation of S_2^{zz}, while the dashed and dotted lines indicate the upper and lower threshold behaviour respectively, fitted using the second method (see main text).

A Elliptic Functions

In this appendix, we collect together the notational conventions and identities for the various elliptic functions that we use in the paper. Many further properties of elliptic functions can be found for example in [63]. We firstly make use of the Jacobi elliptic functions defined by

$$\mathrm{sn}(u) = \sin(\mathrm{am}(u)), \quad \mathrm{cn}(u) = \cos(\mathrm{am}(u)), \quad \mathrm{dn}(u) = \sqrt{1 - k^2 \sin^2(\mathrm{am}(u))}, \tag{A.1}$$

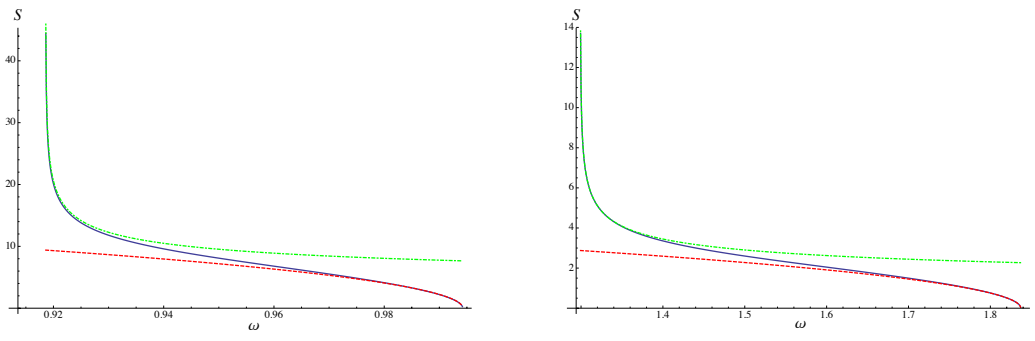

(a) $k/2\pi = 0.125$ (b) $k/2\pi = 0.25$

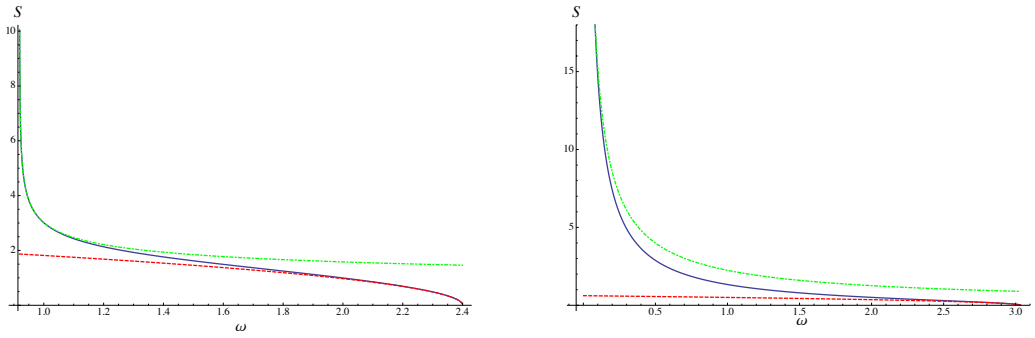

(c) $k/2\pi = 0.375$ (d) $k/2\pi = 0.5$

Figure 9: Threshold behaviour for $\Delta = 0.5$, the solid line is the numerical evaluation of S_2^{zz}, while the dashed and dotted lines indicate the upper and lower threshold behaviour respectively, fitted using the second method (see main text).

where $\mathrm{am}(u)$ is the amplitude function defined in terms of the elliptic modulus k by

$$u = \int_0^{\mathrm{am}(u)} \frac{dx}{\sqrt{1 - k^2 \sin^2(x)}}. \tag{A.2}$$

Defining the conjugate modulus by $k' = \sqrt{1 - k^2}$, the complete elliptic integrals K, and K' are defined in terms of the same modulus k by the integrals:

$$K = \int_0^{\frac{\pi}{2}} \frac{dx}{\sqrt{1 - k^2 \sin^2(x)}}, \quad K' = \int_0^{\frac{\pi}{2}} \frac{dx}{\sqrt{1 - k'^2 \sin^2(x)}}. \tag{A.3}$$

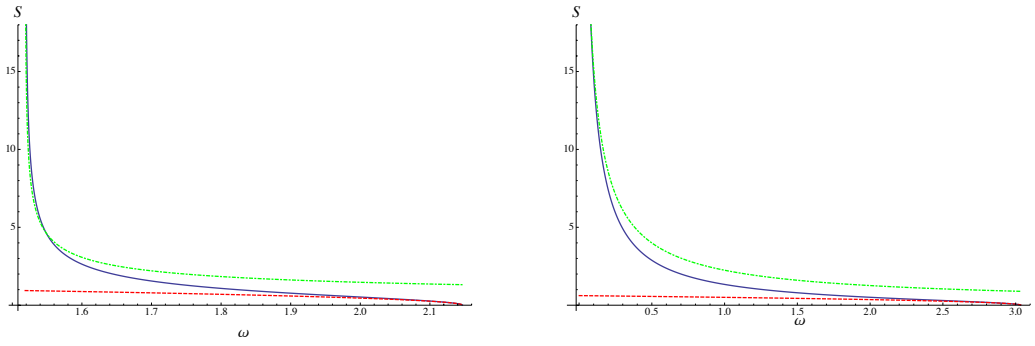

(a) $k/2\pi = 0.125$ (b) $k/2\pi = 0.25$

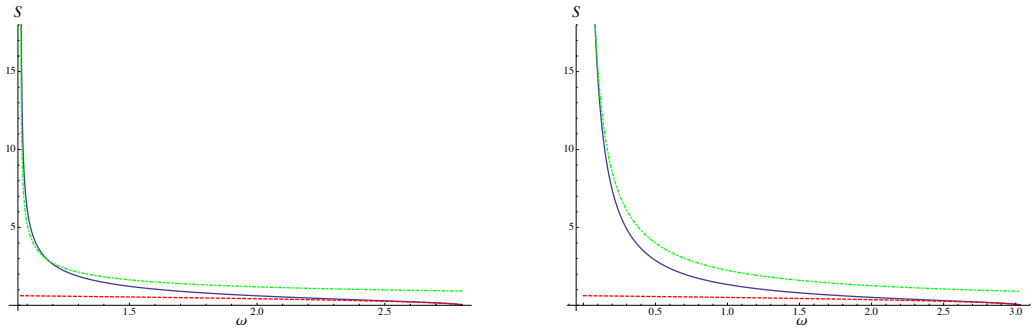

(c) $k/2\pi = 0.375$ (d) $k/2\pi = 0.5$

Figure 10: Threshold behaviour for $\Delta = 0.9$, the solid line is the numerical evaluation of S_2^{zz}, while the dashed and dotted lines indicate the upper and lower threshold behaviour respectively, fitted using the second method (see main text).

We sometimes make the k dependence of these various functions explicit by writing them as $\mathrm{am}(u,k)$, $\mathrm{sn}(u,k)$, $\mathrm{cn}(u,k)$ and $\mathrm{dn}(u,k)$. We also define the following functions

$$\mathrm{snh}(u) = -i\,\mathrm{sn}(iu), \quad \mathrm{cnh}(u) = \mathrm{cn}(iu), \quad \mathrm{dnh}(u) = \mathrm{dn}(iu). \tag{A.4}$$

The other type of elliptic function we use are theta functions. These are defined in terms of a

parameter q called the elliptic nome by

$$\begin{aligned}
\vartheta_1(u,q) &= 2q^{1/4}(q^2;q^2)_\infty \sin(\pi u)\prod_{n=1}^{\infty}(1-2q^{2n}\cos(2\pi u)+q^{4n}) \\
\vartheta_2(u,q) &= 2q^{1/4}(q^2;q^2)_\infty \cos(\pi u)\prod_{n=1}^{\infty}(1+2q^{2n}\cos(2\pi u)+q^{4n}) \\
\vartheta_3(u,q) &= (q^2;q^2)_\infty \prod_{n=1}^{\infty}(1+2q^{2n-1}\cos(2\pi u)+q^{4n-2}) \\
\vartheta_4(u,q) &= (q^2;q^2)_\infty \prod_{n=1}^{\infty}(1-2q^{2n-1}\cos(2\pi u)+q^{4n-2})
\end{aligned}$$

If we identify the elliptic nome as $q = e^{-\pi\frac{K'}{K}}$, then the Jacobi elliptic functions and theta functions are related by

$$\mathrm{sn}(u) = \frac{1}{\sqrt{k}}\frac{\vartheta_1\left(\frac{u}{2K},q\right)}{\vartheta_4\left(\frac{u}{2K},q\right)}, \quad \mathrm{cn}(u) = \frac{\sqrt{k'}}{\sqrt{k}}\frac{\vartheta_2\left(\frac{u}{2K},q\right)}{\vartheta_4\left(\frac{u}{2K},q\right)}, \quad \mathrm{dn}(u) = \sqrt{k'}\frac{\vartheta_3\left(\frac{u}{2K},q\right)}{\vartheta_4\left(\frac{u}{2K},q\right)}.$$

In this paper, we use various identities that we now list.

Identity 1 - the conjugate modulus transformation for Jacobi elliptic functions [63]:

$$\mathrm{sn}(iu,k) = i\frac{\mathrm{sn}(u,k')}{\mathrm{cn}(u,k')}, \quad \mathrm{cn}(iu,k) = i\frac{1}{\mathrm{cn}(u,k')}, \quad \mathrm{dn}(iu,k) = i\frac{\mathrm{dn}(u,k')}{\mathrm{cn}(u,k')}. \tag{A.5}$$

Identity 2 - the half-period property of theta functions [63]:

$$\begin{aligned}
&\vartheta_a(u\pm\frac{\tau}{2},q) = (\pm i)^{g_a}e^{-i\pi\tau/4}e^{\mp i\pi u}\vartheta_{\bar{a}}(u,q), \\
&\text{where } \; q = e^{i\pi\tau} \;\text{ and }\; \bar{1}:=4,\ \bar{2}:=3,\ \bar{3}:=2,\ \bar{4}:=1, \quad g_1=g_4=1,\ g_2=g_3=0.
\end{aligned} \tag{A.6}$$

Identity 3 - [64]:

$$i\frac{\vartheta_1\left(\frac{1}{4}-\frac{i\theta}{\pi},p^{\frac{r}{4}}\right)}{\vartheta_1\left(\frac{1}{4}+\frac{i\theta}{\pi},p^{\frac{r}{4}}\right)} = \mathrm{sn}\left(\frac{2I'\theta}{\pi},k_I\right) + i\,\mathrm{cn}\left(\frac{2I'\theta}{\pi},k_I\right). \tag{A.7}$$

Identity 4 - the limiting behaviour of elliptic functions (which follows straight from the above definitions):

$$\mathrm{am}(u,k=1) = 2\arctan(e^u) - \frac{\pi}{2}. \tag{A.8}$$

$$\mathrm{am}(u,k=0) = u, \;\; \mathrm{sn}(u,k=0) = \sin(u), \;\; \mathrm{cn}(u,k=0) = \cos(u), \;\; \mathrm{dn}(u,k=0) = 1. \tag{A.9}$$

B Derivation of (2.25) in the Vertex Operator Picture

A key observation is an identification of the type I vertex operators with the half-transfer matrices on the lattice. Then applying the gauge transformations (2.21) to each R matrix constituting the half-transfer matrix, one can reach the following definition of the type I vertex operators in the disordered regime.

$$\widetilde{\Phi}^{(j)}_{\varepsilon;\ell}(u) := \sum_{\varepsilon'=\pm}(U_{j+\ell})_{\varepsilon\varepsilon'}\mathcal{G}_{j+\ell+1}\Phi^{(\ell,1-\ell)}_{\varepsilon'}(u)\mathcal{G}^{-1}_{j+\ell} \;:\; \mathcal{G}_{j+\ell}\mathcal{H}^{(1-\ell)} \to \mathcal{G}_{j+\ell+1}\mathcal{H}^{(\ell)}. \tag{B.10}$$

Note that from (2.23) these are linear operators on $\mathcal{H}^{(j)}_{dis}$. Accordingly, one can realise a local operator as an operator on $\mathcal{H}^{(j)}_{dis} = \mathcal{G}_{j+\ell}\mathcal{H}^{(1-\ell)}$ by

$$\mathcal{O}'(E_{\varepsilon\varepsilon'})^{(j)}_{\ell} := \widetilde{\Phi}^{(j)}_{-\varepsilon;1-\ell}(u-1)\widetilde{\Phi}^{(j)}_{\varepsilon';\ell}(u)\Big|_{u=0}.$$

Then it follows from (2.9) and (B.10) that we have the gauge transformation of the spin operators as

$$\begin{aligned}
&\mathcal{O}'(\sigma^x)^{(j)}_{\ell} = (-)^{j+\ell}\mathcal{G}_{j+\ell}\mathcal{O}(\sigma^z)^{(1-\ell)}\mathcal{G}^{-1}_{j+\ell}, \qquad \mathcal{O}'(\sigma^y)^{(j)}_{\ell} = \mathcal{G}_{j+\ell}\mathcal{O}(\sigma^x)^{(1-\ell)}\mathcal{G}^{-1}_{j+\ell},\\
&\mathcal{O}'(\sigma^z)^{(j)} = (-)^{j+\ell}\mathcal{G}_{j+\ell}\mathcal{O}(\sigma^y)^{(1-\ell)}\mathcal{G}^{-1}_{j+\ell}.
\end{aligned} \tag{B.11}$$

This is consistent to the transformation of σ^α as a 2×2 matrix: $\mathrm{Ad}U_j^{-1} : \sigma^x, \sigma^y, \sigma^z \mapsto (-1)^j\sigma^z, \sigma^x, (-1)^j\sigma^y$.

In the vertex operator picture, the gauge transformation of the vacuum vectors $|\mathrm{vac}; pr\rangle^{(j)} = x^{2H^{(j)}}/(Z^{(j)})^{1/2} \in \mathcal{F}^{(j)} \cong \mathrm{End}(\mathcal{H}^{(j)})$ follows from the fact that $x^{2H^{(j)}}$ originates as the product of two corner transfer matrices. Hence the vacuum vectors as well as other physical $2n$-spinon excited states should have the same transformation property as the corner transfer matrix. Therefore we identify new vacuum vectors as

$$|\mathrm{vac}\rangle^{(j)} = \mathcal{G}_{j+\ell}\frac{1}{(Z^{(1-\ell)})^{1/2}}x^{2H^{(1-\ell)}}\mathcal{G}^{-1}_{j+\ell} \quad (\ell = 0, 1) \tag{B.12}$$

in $\mathcal{F}^{(j)}_{dis} \cong \mathrm{End}(\mathcal{H}^{(j)}_{dis})$. Similarly to the type I case, the type II vertex operators $\Psi^{*(1-j,j)}_{\varepsilon}(i\theta/\pi)$ in the principal regime are mapped to linear operators on $\mathcal{H}^{(j)}_{dis}$ by

$$\widetilde{\Psi}^{*(j)}_{\varepsilon;\ell}(\theta) = \mathcal{G}_{j+\ell+1}\Psi^{*(\ell,1-\ell)}_{\varepsilon}(i\theta/\pi)\mathcal{G}^{-1}_{j+\ell} \ : \ \mathcal{G}_{j+\ell}\mathcal{H}^{(1-\ell)} \to \mathcal{G}_{j+\ell+1}\mathcal{H}^{(\ell)}.$$

One should note that the new type II vertex operators $\widetilde{\Psi}^{*(j)}_{\varepsilon;\ell}(\theta)$ commute with the new type I vertex operators $\widetilde{\Phi}^{(j)}_{\varepsilon;\ell}(u)$ in pairs. Namely,

$$\widetilde{\Phi}^{(j)}_{\varepsilon;\ell}(u)\widetilde{\Psi}^{*(j)}_{\mu_2;1-\ell}(\theta_2)\widetilde{\Psi}^{*(j)}_{\mu_1;\ell}(\theta_1) = \tau(u - i\theta_1/\pi)\tau(u - i\theta_2/\pi)\widetilde{\Psi}^{*(j)}_{\mu_2;\ell}(\theta_2)\widetilde{\Psi}^{*(j)}_{\mu_1;1-\ell}(\theta_1)\widetilde{\Phi}^{(j)}_{\varepsilon;\ell}(u).$$

Hence we obtain the following identification of the disordered $2n$-spinon states

$$\begin{aligned}
&|\theta_1, \theta_2 \cdots \theta_{2n}\rangle^{(j)}_{\varepsilon_1,\varepsilon_2,\cdots,\varepsilon_{2n}}\\
&= \widetilde{\Psi}^{*(j)}_{\varepsilon_{2n};1-\ell}(\theta_{2n}) \cdots \widetilde{\Psi}^{*(j)}_{\varepsilon_2;1-\ell}(\theta_2)\widetilde{\Psi}^{*(j)}_{\varepsilon_1;\ell}(\theta_1)|\mathrm{vac}\rangle^{(j)}\\
&= \mathcal{G}_{j+\ell}\Psi^{*(1-\ell,\ell)}_{\varepsilon_{2n}}(i\theta_{2n}/\pi)\cdots\Psi^{*(1-\ell,\ell)}_{\varepsilon_2}(i\theta_2/\pi)\Psi^{*(\ell,1-\ell)}_{\varepsilon_1}(i\theta_1/\pi)\frac{1}{(Z^{(1-\ell)})^{1/2}}x^{2H^{(1-\ell)}}\mathcal{G}^{-1}_{j+\ell}.
\end{aligned} \tag{B.13}$$

Combining (B.11), (B.12) and (B.13), we then obtain the form factor of the spin operator σ^α in the disordered regime as

$$\begin{aligned}
&{}^{(j)}\langle\mathrm{vac}|\sigma^\alpha|\theta_1, \cdots, \theta_{2n}\rangle^{(j)}_{\varepsilon_1,\cdots,\varepsilon_{2n}}\\
&= \frac{1}{Z^{(1-\ell)}}\mathrm{tr}_{\mathcal{H}^{(j)}_{dis}}(\mathcal{G}_{j+\ell}x^{2H^{(1-\ell)}}\mathcal{G}^{-1}_{j+\ell}\mathcal{O}'(\sigma^\alpha)^{(j)}\widetilde{\Psi}^{*(j)}_{\varepsilon_{2n};1-\ell}(\theta_{2n})\widetilde{\Psi}^{*(j)}_{\varepsilon_{2n-1};\ell}(\theta_{2n-1})\cdots\widetilde{\Psi}^{*(j)}_{\varepsilon_1;\ell}(\theta_1)\mathcal{G}_{j+\ell}x^{2H^{(1-\ell)}}\mathcal{G}^{-1}_{j+\ell})\\
&= \frac{1}{Z^{(1-\ell)}}\mathrm{tr}_{\mathcal{H}^{(1-\ell)}}(x^{4H^{(1-\ell)}}\mathcal{O}(\mathrm{Ad}U^{-1}_{j+\ell}(\sigma^\alpha))^{(1-\ell)}\Psi^{*(1-\ell,\ell)}_{\varepsilon_{2n}}(i\theta_{2n}/\pi)\Psi^{*(\ell,1-\ell)}_{\varepsilon_{2n-1}}(i\theta_{2n-1}/\pi)\cdots\Psi^{*(\ell,1-\ell)}_{\varepsilon_1}(i\theta_1/\pi))\\
&= {}^{(1-\ell)}\langle\mathrm{vac}; pr|\mathrm{Ad}U^{-1}_{j+\ell}(\sigma^\alpha)|\theta_1, \cdots, \theta_{2n}; pr\rangle^{(1-\ell)}_{\varepsilon_1,\cdots,\varepsilon_{2n}}
\end{aligned} \tag{B.14}$$

with $\ell = 0, 1$.

References

[1] T. Giamarchi. *Quantum Physics in One Dimension*. Oxford University Press, 2004.

[2] W. Heisenberg. Zur Theorie des Ferromagnetismus. *Z. Phys.*, 49:619, 1928.

[3] R. Orbach. Linear antiferromagnetic chain with anisotropic coupling. *Phys. Rev.*, 112(2):309–316, 1958.

[4] M. Takahashi. *Thermodynamics of one-dimensional solvable models*. Cambridge University Press, Cambridge, 1999.

[5] B. M. McCoy. *Advanced statistical mechanics*, volume 146 of *International Series of Monographs on Physics*. Oxford University Press, Oxford, 2010.

[6] J. P. Goff, D. A. Tennant, and S. E. Nagler. Exchange mixing and soliton dynamics in the quantum spin chain $CsCoCl_3$. *Phys. Rev. B*, 52(22):15992–16000, 1995.

[7] K. Totsuka. Magnetization plateau in the $S = 1/2$ Heisenberg spin chain with next-nearest-neighbor and alternating nearest-neighbor interactions. *Phys. Rev. B*, 57(6):3454–3465, 1998.

[8] B. C. Watson et al. Magnetic Spin Ladder $(C_5H_{12}N)_2CuBr_4$: High-Field Magnetization and Scaling near Quantum Criticality. *Phys. Rev. Lett.*, 86(22):5168–5171, 2001.

[9] B. Thielemann et al. Direct Observation of Magnon Fractionalization in the Quantum Spin Ladder. *Phys. Rev. Lett.*, 102:107204, 2009.

[10] A. B. Kuklov and B. V. Svistunov. Counterflow Superfluidity of Two-Species Ultracold Atoms in a Commensurate Optical Lattice. *Phys. Rev. Lett.*, 90(10):100401, 2003.

[11] L.-M. Duan, E. Demler, and M. D. Lukin. Controlling Spin Exchange Interactions of Ultracold Atoms in Optical Lattices. *Phys. Rev. Lett.*, 91(9):090402, 2003.

[12] J. J. Garcia-Ripoll and J. I. Cirac. Spin dynamics for bosons in an optical lattice. *New Jour. Phys.*, 5(1):76, 2003.

[13] M. Lewenstein, A. Sanpera, V. Ahufinger, B. Damski, A. Sen, and U. Sen. Ultracold atomic gases in optical lattices: mimicking condensed matter physics and beyond. *Adv. Phys.*, 56:243, 2007.

[14] Y.-A. Chen, S. Nascimbène, M. Aidelsburger, M. Atala, S. Trotzky, and I. Bloch. Controlling Correlated Tunneling and Superexchange Interactions with AC-Driven Optial Lattices. 2011. arXiv:1104.1833.

[15] J.-S. Caux, H. Konno, M. Sorrell, and R. Weston. Tracking the Effects of Interactions on Spinons in Gapless Heisenberg Chains. *Phys. Rev. Lett.*, 106(21):217203, 2011.

[16] F. D. M. Haldane. 'Luttinger liquid theory' of one-dimensional quantum fluids. I. Properties of the Luttinger model and their extension to the general 1D interacting spinless Fermi gas. *J. Phys C: Sol. St. Phys.*, 14(19):2585, 1981.

[17] F. D. M. Haldane. Demonstration of the "Luttinger liquid" character of Bethe-ansatz-soluble models of 1-d quantum fluids. *Phys. Lett. A*, 81(2-3):153 – 155, 1981.

[18] L. D. Faddeev and L. A. Takhtajan. What is the spin of a spin wave ? *Phys. Lett. A*, 85:375, 1981.

[19] A. Furrer, J. Mesot, and T. Strässle. *Neutron Scattering in Condensed Matter Physics*. World Scientific, 2009.

[20] M. Jimbo and T. Miwa. *Algebraic Analysis of Solvable Lattice Models*. CBMS Regional Conference Series in Mathematics, vol. 85. Amer. Math. Soc., 1994.

[21] A. H. Bougourzi, M. Couture, and M. Kacir. Exact two-spinon dynamical correlation function of the one-dimensional Heisenberg model. *Phys. Rev. B*, 54(18):R12669–R12672, 1996.

[22] M. Karbach, G. Müller, A. H. Bougourzi, A. Fledderjohann, and K.-H. Mütter. Two-spinon dynamic structure factor of the one-dimensional $s = 1/2$ Heisenberg antiferromagnet . *Phys. Rev. B*, 55(18):12510–12517, 1997.

[23] A. Abada, A. H. Bougourzi, and B. Si-Lakhal. Exact four-spinon dynamical correlation function of the Heisenberg model. *Nucl. Phys. B*, 497(3):733 – 753, 1997.

[24] J.-S. Caux and R. Hagemans. The four-spinon dynamical structure factor of the Heisenberg chain. *J. Stat. Mech: Th. Exp.*, page P12013, 2006.

[25] A. H. Bougourzi, M. Karbach, and G. Müller. Exact two-spinon dynamic structure factor of the one-dimensional $s = 12$ Heisenberg-Ising antiferromagnet. *Phys. Rev. B*, 57(18):11429–11438, 1998.

[26] J.-S. Caux, J. Mossel, and I. Pérez Castillo. The two-spinon transverse structure factor of the gapped Heisenberg antiferromagnetic chain. *J. Stat. Mech.: Th. Exp.*, 2008(08):P08006, 2008.

[27] M. Jimbo, H. Konno, and T. Miwa. Massless XXZ model and degeneration of the elliptic algebra $\mathcal{A}_{q,p}(\widehat{\mathfrak{sl}}_2)$. *Deformation theory and symplectic geometry*, pages 117–138, 1997.

[28] M. Jimbo, T. Miwa, and A. Nakayashiki. Difference Equations for the Correlation Functions of the Eight-Vertex Model. *J. Phys.*, A26:2199–2209, 1993.

[29] M. Jimbo, R. Kedem, H. Konno, T. Miwa, and R.A. Weston. Difference equations in spin chains with a boundary. *Nucl. Phys.*, B448:429–456, 1995.

[30] O. Foda, K. Iohara, M. Jimbo, R. Kedem, T. Miwa, and H. Yan. An elliptic quantum algebra for $\widehat{sl}_2$. *Lett. Math. Phys.*, 32:259–268, 1994.

[31] O. Foda, K. Iohara, M. Jimbo, R. Kedem, T. Miwa, and H. Yan. Notes on highest weight modules of the elliptic algebra $\mathcal{A}_{q,p}(\widehat{\mathfrak{sl}}_2)$. *Progr. Theoret. Phys. Suppl.*, (118):1–34, 1995. Quantum field theory, integrable models and beyond (Kyoto, 1994).

[32] M.Jimbo, H.Konno, S.Odake, and J.Shiraishi. Quasi-Hopf twistors for elliptic quantum groups. *Transformation Groups*, 4:303–327, 1999.

[33] R. Baxter. *Exactly Solved Models in Statistical Mechanics*. Academic Press, 1982.

[34] H. Konno. An Elliptic Algebra $U_{q,p}(\widehat{\mathfrak{sl}}_2)$ and the Fusion RSOS Model. *Comm. Math. Phys.*, 195:373–403, 1998.

[35] M. Jimbo, H. Konno, S. Odake, and J. Shiraishi. Elliptic algebra $U_{q,p}(\widehat{\mathfrak{sl}}_2)$: Drinfeld currents and vertex operators. *Comm. Math. Phys.* , 199:605–647, 1999.

[36] H. Konno. Elliptic Quantum Group $U_{q,p}(\widehat{\mathfrak{sl}}_2)$, Hopf Algebroid Structure and Elliptic Hypergeometric Series. *J. Geom. Phys.*, 59:1485–1511, 2009.

[37] M. Lashkevich and Y. Pugai. Free field construction for correlation functions of the eight-vertex model. *Nuclear Phys. B*, 516(3):623–651, 1998.

[38] M. Lashkevich. Free field construction for the eight-vertex model: representation for form factors. *Nuclear Phys. B*, 621(3):587–621, 2002.

[39] T. Kojima, H. Konno, and R. Weston. The vertex-face correspondence and correlation functions of the fusion eight-vertex model. I. The general formalism. *Nuclear Phys. B*, 720(3):348–398, 2005.

[40] M. Jimbo and T. Miwa. q-KZ equation with $|q| = 1$ and correlation functions of the XXZ model in the gapless regime. *J. Phys.*, A29:2923–2958, 1996.

[41] S. Lukyanov and V. Terras. Long-distance asymptotics of spin-spin correlation functions for the XXZ spin chain. *Nuclear Phys. B*, 654(3):323–356, 2003.

[42] B. Davies, O. Foda, M. Jimbo, T. Miwa, and A. Nakayashiki. Diagonalization of the XXZ Hamiltonian by Vertex Operators. *Comm. Math. Phys.*, 151:89–153, 1993.

[43] J. D. Johnson, S. Krinsky, and B. M. McCoy. Vertical-arrow correlation length in the eight-vertex model and the low-lying excitations of the XYZ hamiltonian. *Phys. Rev.*, A8:2526–2547, 1973.

[44] S. Lukyanov and Y. Pugai. Multi-point local height probabilities in the integrable RSOS model. *Nuclear Phys. B*, 473(3):631–658, 1996.

[45] T. Miwa and R. Weston. Boundary ABF models. *Nuclear Phys. B*, 486(3):517–545, 1997.

[46] Th. Niemeijer. Some exact calculations on a chain of spins. *Physica*, 36(3):377 – 419, 1967.

[47] S. Katsura, T. Horiguchi, and M. Suzuki. Dynamical properties of the isotropic XY model. *Physica*, 46(1):67 – 86, 1970.

[48] G. Müller, H. Thomas, M. W. Puga, and H. Beck. Quantum spin dynamics of the one-dimensional planar antiferromagnet. *J. Phys. C: Sol. St. Phys.*, 14(23):3399, 1981.

[49] P. C. Hohenberg and W. F. Brinkman. Sum rules for the frequency spectrum of linear magnetic chains. *Phys. Rev. B*, 10(1):128–131, 1974.

[50] C. N. Yang and C. P. Yang. One-dimensional chain of anisotropic spin-spin interactions. ii. properties of the ground-state energy per lattice site for an infinite system. *Phys. Rev.*, 150(1):327–339, 1966.

[51] J.-S. Caux and J. M. Maillet. Computation of Dynamical Correlation Functions of Heisenberg Chains in a Magnetic Field. *Phys. Rev. Lett.*, 95(7):077201, Aug 2005.

[52] J.-S. Caux, R. Hagemans, and J. M. Maillet. Computation of dynamical correlation functions of Heisenberg chains: the gapless anisotropic regime. *J. Stat. Mech.: Th. Exp.*, 2005(09):P09003, 2005.

[53] A. Imambekov and L. I. Glazman. Exact Exponents of Edge Singularities in Dynamic Correlation Functions of 1D Bose Gas. *Physical Review Letters*, 100(20):206805, 2008.

[54] A. Imambekov and L. I. Glazman. Universal Theory of Nonlinear Luttinger Liquids. *Science*, 323(5911):228–231, 2009.

[55] L. I. Glazman A. Imambekov, T. L. Schmidt. One-Dimensional Quantum Liquids: Beyond the Luttinger Liquid Paradigm. 2011. arXiv:1110.1374.

[56] M. Pustilnik, M. Khodas, A. Kamenev, and L. I. Glazman. Dynamic response of one-dimensional interacting fermions. *Phys. Rev. Lett.*, 96(19):196405, 2006.

[57] R. G. Pereira, J. Sirker, J.-S. Caux, R. Hagemans, J. M. Maillet, S. R. White, and I. Affleck. Dynamical spin structure factor for the anisotropic spin-1/2 Heisenberg chain. *Phys. Rev. Lett.*, 96(25):257202, Jun 2006.

[58] M. Khodas, M. Pustilnik, A. Kamenev, and L. I. Glazman. Fermi-luttinger liquid: Spectral function of interacting one-dimensional fermions. *Phys. Rev. B*, 76(15):155402, 2007.

[59] R. G. Pereira, J. Sirker, J.-S. Caux, R. Hagemans, J. M. Maillet, S. R. White, and I. Affleck. Dynamical structure factor at small q for the XXZ spin-1/2 chain. *J. Stat. Mech.: Th. Exp.*, 2007(08):P08022, 2007.

[60] V. V. Cheianov and M. Pustilnik. Threshold Singularities in the Dynamic Response of Gapless Integrable Models. *Phys. Rev. Lett.*, 100(12):126403, 2008.

[61] R. G. Pereira, S. R. White, and I. Affleck. Exact Edge Singularities and Dynamical Correlations in Spin-1/2 Chains. *Phys. Rev. Lett.*, 100(2):027206, 2008.

[62] R. G. Pereira, S. R. White, and I. Affleck. Spectral function of spinless fermions on a one-dimensional lattice. *Phys. Rev. B*, 79(16):165113, 2009.

[63] I. S. Gradshteyn and I. M. Ryzhik. *Table of integrals, series, and products.* Academic Press Inc., San Diego, CA, sixth edition, 2000.

[64] E. T. Whittaker and G. N. Watson. *A course of modern analysis.* Cambridge Mathematical Library. Cambridge University Press, Cambridge, 1996.